

**Diffusion coefficient of charge carriers in disordered
semiconductors retaining a combination of exponential and
Gaussian mobility-gap states: application to amorphous selenium**

Dilshad Hossain

A Thesis
in
the Department
of
Electrical and Computer Engineering

Presented in Partial Fulfillment of the Requirement
for the Degree of
Master of Applied Science in Electrical and Computer Engineering

Concordia University
Montréal, Québec, Canada

March 2022

© Dilshad Hossain, 2022

CONCORDIA UNIVERSITY
School of Graduate Studies

This is to certify that the thesis prepared

By: Dilshad Hossain

Entitled: Diffusion coefficient of charge carriers in disordered semiconductors retaining a combination of exponential and Gaussian mobility-gap states: application to amorphous selenium

and submitted in partial fulfillment of the requirements for the degree of

Master of Applied Science (Electrical and Computer Engineering)

complies with the regulations of the University and meets the accepted standards with respect to originality and quality.

Signed by the final examining committee:

_____ Chair
Dr. Pouya Valizadeh

_____ Examiner
Dr. Amr Youssef (CIISE)

_____ Examiner
Dr. Pouya Valizadeh

_____ Thesis Supervisor
Dr. M. Z. Kabir

Approved by: _____

Dr. Yousef R. Shayan, Chair
Department of Electrical and Computer Engineering

Dr. Mourad Debbabi, Dean, Gina Cody School of Engineering and Computer

Date: _____

Abstract

Diffusion coefficient of charge carriers in disordered semiconductors retaining a combination of exponential and Gaussian mobility-gap states: application to amorphous selenium

Dilshad Hossain

Charge carrier transport in disordered semiconductors is highly influenced by the defect states near the mobility edges. The ratio of the diffusion coefficient and drift mobility in crystalline semiconductor under a wide range of carrier concentration can conveniently be calculated by the Einstein relation. The density of states (DOS) in the mobility gap in amorphous/disordered semiconductors can change the generalized Einstein relation. It has been found that the ratio of the diffusion coefficient and drift mobility is larger than the conventional Einstein relation even at the presence of lower carrier concentration than the degenerate limit. A theoretical model for the generalized Einstein relation (GER), namely, the diffusivity-mobility ratio, for disordered semiconductors retaining a combination of exponential and Gaussian mobility-gap states with square-root distribution of extended states, is presented in this thesis work. The conditions for determining the diffusion coefficient of charge carriers from Einstein relation are described in the thesis work. The effects of various parameters constituting the density of states (DOS) distribution on the Einstein relation are examined. The results show that the diffusivity-mobility ratio for such DOS distribution substantially deviates from traditional constant value for carrier

concentration larger than 10^{10} cm^{-3} . The value of diffusivity-mobility ratio strongly depends on the amount, energy position and the shape of the Gaussian peaks.

The diffusion coefficient determined from Einstein relation in amorphous semiconductors is valid at equilibrium transport when the electric field is very low. Under applied field, charge carriers undergo many trapping-detrapping events in the energy distributed mobility gap states during their travel. The statistical variations of the trapping and release times create a considerable spreading of signal. Thus, the actual diffusion coefficient appears to be much larger than it should be from the known Einstein relation. The additional diffusion coefficient due to multiple trapping in disordered semiconductors (namely field diffusion) under quasi-equilibrium transport is also examined as a function of electric field and carrier concentration.

Acknowledgement

My humblest gratitude to all those who extended their help, directly and indirectly, throughout this research. Primarily, I would like to express my earnest gratitude to my supervisor Dr. M. Z. Kabir for this opportunity, his continued guidance, motivation, and financial support throughout this work, without which this would not have been possible. I am also grateful to my parents and my husband who supported me mentally through their continuous encouragement. Last but not the least, I would like to acknowledge the friendly conversations, and advice of my colleague Mr. Mithun Roy.

Table of Contents

List of Figures	viii
List of Tables	x
List of Abbreviations	xi
List of Symbols	xii
Chapter 1: Introduction	1
1.1 Semiconductor	1
1.2 Types of Semiconductors	2
1.2.1 Degenerate vs Nondegenerate Semiconductors	2
1.2.2 Crystalline vs Amorphous Semiconductor	3
1.2.3 Amorphous Semiconductor	4
1.3 Research motivation	7
1.3.1 Conventional Einstein Relation (CER)	7
1.3.2 Deviation from Conventional Einstein Relation (CER)	8
1.4 Research Objectives	11
1.5 Thesis Outline	11
Chapter 2: Amorphous Selenium	13
2.1 Introduction	13
2.2 Carrier Statistics in Non-degenerate and Degenerate Semiconductors in Thermal Equilibrium	13
2.3 Amorphous Selenium	16
2.3.1 Uses of Amorphous Selenium	17
2.4 Density of States of a-Se	18
Chapter 3: Modeling of Diffusion Coefficient in Disordered Semiconductors	23
3.1 Introduction	23
3.2 Charge Carrier Transport Under Multiple Trapping	23
3.3 Modeling Diffusion Coefficient from GER	28
3.4 Developing Field Diffusion Coefficient Under Quasi-Equilibrium Transport	31
3.5 Effective Drift mobility for a-Se at High Electric Field	36
3.6 Conclusion	37
Chapter 4: Result and discussion	38
4.1 Introduction	38

4.2 Diffusion coefficient from Einstein relation	38
4.3 Field-Diffusion Under Quasi-Equilibrium Transport	46
4.4 Conclusion.....	50
Chapter 5: Conclusions and Contributions	51
5.1 Conclusions	51
5.2 Contributions.....	51
5.3 Future works.....	52
5.4 Publication.....	52
References.....	53

List of Figures

Figure	Page
Fig. 1.1: Atomic arrangement in (a) Crystalline semiconductor (b) Amorphous semiconductor	4
Fig. 1.2: (a) Energy band diagram of crystalline semiconductor. (b) DOS model proposed by Mott for amorphous semiconductor. (c) The CFO model for amorphous semiconductors. (d) Deep localized states proposed by Marshall and Owen	6
Fig. 2.1: The localized density-of-states distribution in a-Se according to the Abkowitz model	19
Fig. 4.1: The variation of normalized ratio D_e/μ_e as a function of the free electron concentration for different ΔE_m	41
Fig. 4.2: The variation of normalized ratio D_e/μ_e as a function of the free electron concentration for different g_c	42
Fig. 4.3: The variation of normalized ratio D_e/μ_e as a function of the free electron concentration for different N_m	43
Fig. 4.4: The variation of the normalized ratio D_e/μ_e with the Fermi-level for different positions of Gaussian peak near conduction band	44
Fig. 4.5: The variation on normalized D_e/μ_e ratio with electron concentration using parameters specified by Abkowitz and Kasap <i>et al.</i>	45
Fig. 4.6: The variation on normalized D_h/μ_h ratio with hole concentration using parameters specified by Abkowitz and Benkhedir <i>et al.</i>	46

Fig. 4.7: Normalized field-diffusion coefficient of electrons in a-Se as a function of electron concentration at three different electric fields	48
Fig. 4.8: Normalized total diffusion coefficient of electrons in a-Se as a function of electric field at three different electron concentrations	49
Fig. 4.9: Normalized field-diffusion coefficient of holes in a-Se as a function of hole concentration at three different electric fields	50
Fig. 4.10: Normalized total diffusion coefficient of holes in a-Se as a function of electric field at three different hole concentrations	51

List of Tables

Table	Page
Table I: DOS below conduction-band mobility edge, E_c in the mobility gap	21
Table II: DOS above valence-band mobility edge, E_v in the mobility gap	22

List of Abbreviations

a-Se	Amorphous Selenium
DOS	Density of States
ER	Einstein Relation
IC	Integrated Circuit
CER	Conventional Einstein Relation
GER	Generalized Einstein Relation
FDC	Field Diffusion Coefficient

List of Symbols

$g(E)$	-	Density of States of a-Se at energy E
N_m	-	Peak value of shallow traps
E_c	-	Conduction band mobility edge
g_c	-	Density of states at conduction band
$g_s(E)$	-	Density of states function at conduction band edge
ΔE_m	-	Width of Gaussian peak
T_0	-	Characteristic temperature
γ_c	-	Decay rate of exponential tail states in mobility gap
t	-	Time
n	-	Total electron concentration
n_c	-	Electron concentration in the extended states
μ_{0e}	-	Drift mobility of electron at extended states
μ_e	-	Effective drift mobility of electron
D_{0e}	-	Diffusion coefficient of electron at extended states
D_e	-	Effective diffusion of electron
D_{fe}	-	Field diffusion coefficient

N_t	-	Trapped electron concentration
ν	-	Attempt to escape frequency
C_t	-	Capture coefficient of free electron
J_{dr}	-	Drift current of electron
J_d	-	Diffusion current of electron
e	-	Electron charge
F	-	Electric field
E_{Fn}	-	Quasi fermi energy of electron
k	-	Boltzmann constant
E_c	-	Energy at conduction band
E_v	-	Energy at valance band

Chapter 1: Introduction

1.1 Semiconductor

A Semiconductor is a material which has conductivity level higher than an insulator but less than a conductor. Semiconductor responds to external forces such as temperature, electric field, light etc. which allows manipulation of the conductivity levels. The conductivity level of a semiconductor can also be changed by adding doping.

Semiconductor can handle wide range of current-voltage limit which makes it ideal for various complex designs in electronic systems. Since the electrical properties of semiconductor can be modified by external means, devices made from semiconductor can be used for switching, energy conversion and amplification. In practice, they are used widely to produce various compact, reliable, power efficient devices including MOSSFET, solar cell, computer, appliance, medical equipment, smartphone, automobile etc.

Interests in semiconductor can be traced back to nineteenth century when Michael Faraday investigated the temperature dependence of the electrical conductivity of silver sulphide in 1833. Two major discoveries in the 1870s led to the development of the 1st semiconductor device: discovery of the photoconductivity of selenium in 1873 by Willoughby Smith whilst working on submarine cables and the discovery of electricity production in a selenium device when light was shone on it in 1876 by William Grylls Adams and Richard Evans Day [1].

In 1906, Greenleaf Whittier Pickard filed and obtained patent for crystal silicon detector (earliest stage of diode detector) [2] and, in 1947, the first transistor was constructed and tested at Bell Telephone Laboratories by William Shockley, John Bardeen, and Walter Brattain [2].

In mid 1960s practical MOS transistors were developed. The MOS technologies, especially CMOS, become the backbone of modern IC design and development, which can store information, and can perform arithmetic and logic on semiconductor chip. The development of the integrated circuits and their wide-range use has led to significant improvements in the production of electronic devices.

1.2 Types of Semiconductors

Different types of semiconductors are used for different purposes. Based on the relative amount of free carrier concentration, they can be divided into two categories: degenerate and nondegenerate semiconductors. They can also be classified based on the periodic order of atomic arrangement: crystalline, polycrystalline, and amorphous semiconductors.

1.2.1 Degenerate vs Nondegenerate Semiconductors

The electronic and optical properties of semiconductor materials are highly responsive to impurities, which may be added in precisely controlled amounts. Such impurities are used to vary the conductivities of semiconductors over wide ranges. For example, an impurity concentration of one part per million can change a sample of Si from a poor conductor to a good conductor. This process of controlled addition of impurities is called doping [3]. Based on the level of doping, semiconductors can be divided into two primary categories: degenerate and nondegenerate semiconductor.

When doping level is adequately high for the semiconductor to act like metal, it is called degenerate semiconductor. Adding high impurity into semiconductor improves the interaction

between dopant atoms, which generates a band of donor/acceptor energy levels rather than a single discrete energy level. The energy bands can overlap with the corresponding band edges of conduction and valence band. Because of the overlapping, the Fermi level enters conduction band (in case of *n*-type semiconductor) or valence band (in case of *p*-type semiconductor) [3].

On the contrary, when the doping level in the semiconductors is low enough to maintain the Fermi level in the forbidden band gap and not closer than $3kT$ from the band edges, they are called non-degenerate semiconductors [3].

1.2.2 Crystalline vs Amorphous Semiconductor

Based on the nature of atomic arrangement with their neighbouring atoms, semiconductors can be divided into three categories: Crystalline, Polycrystalline and Amorphous semiconductors. Crystalline semiconductors are those which have long-range order, i.e., atoms are arranged in a regular, periodical, and repeated structure throughout the material. Polycrystalline semiconductors are composed of many small crystals with random orientation.

Conversely, a material is called amorphous material when they lack long-range order throughout the whole structure. Such materials are created when they are cooled down rapidly, which prevents them from achieving the minimum thermal energy at a specific bond radius (lattice point) and locks the atoms in a disorderly arrangement throughout the material. Lower mobility in liquid state of a material or complex structure in atomic level makes it difficult for crystallization, making it easier to be amorphous.

As amorphous semiconductors do not have long-range order and lack periodical or repeated structure like crystalline semiconductors, they show small or short-range order which can be used as a thin film over large areas that are usually used in photovoltaic technology, x-ray detectors, printers etc. However, because of the lack of periodicity, the density of states (DOS) is more complex than crystalline semiconductors. Figure 1.1 shows the different atomic arrangement between crystalline and amorphous semiconductor.

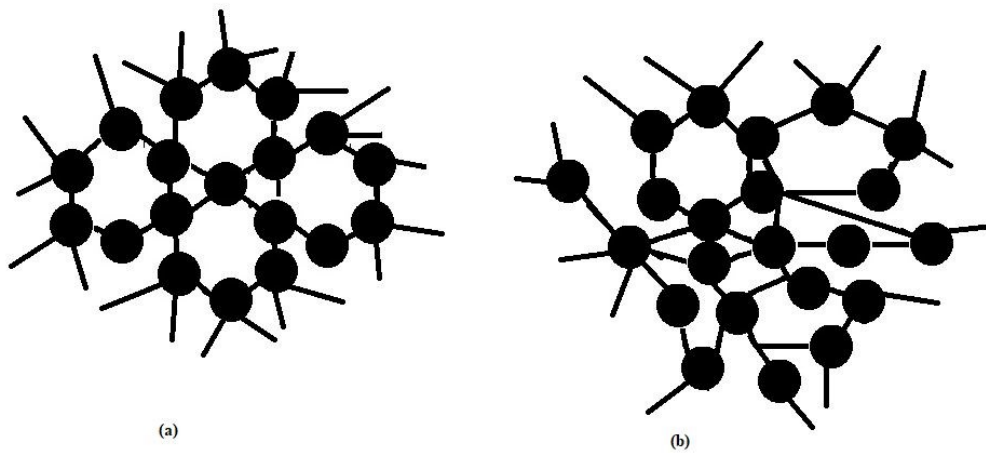


Fig 1.1: Atomic arrangement in (a) Crystalline semiconductor (b) Amorphous semiconductor [4].

1.2.3 Amorphous Semiconductor

After the development of quantum mechanics in 1920s and 1930s it was readily applied to the study of crystalline solid because of its periodic structure. Due to the complexities of the application of quantum mechanics to non-periodic structures, the same did not happen to amorphous semiconductors. The theoretical understanding of the properties of amorphous materials started in 1960s which has resulted in more prominent use since 2000s because of their

significant higher level of diversities in their physical properties. Moreover, the preparation of amorphous materials usually does not require the same carefully controlled growth techniques providing a robust economical advantage for many applications [5].

When atoms are cooled to form solid structures, the individual atomic electron energy states interact with each other and form a series of allowed and forbidden band of energy states. However, there are finite number of states in conduction and valence bands, which is expressed by the term density of states (DOS). At any energy level, DOS is represented as $g(E)$. Crystalline materials have very well-defined DOS which include forbidden band gap (where no electron is allowed at thermal equilibrium), valance band and conduction band.

Unlike perfect crystalline materials, amorphous materials lack long-range order, which makes the band model of amorphous semiconductor more complicated. However, even though they are random in long distance, they have similar structure with neighbouring atoms with local bonding, which causes an optical gap like crystalline materials [6]. Due to short-range order, amorphous semiconductors have spatial vibrations in bond lengths and angles causing random fluctuations in potential energy of electrons throughout the whole sample which leads to defects in their band gap.

Instead of sharp band edge like crystalline material, amorphous material has mobility edges which separates their localized states from their extended states. The distance between two mobility edges is called the mobility gap. The charge carriers can be trapped in the defect states

and released from there by thermal energy [7]. Figure 1.2 represents energy band diagram of crystalline and amorphous semiconductors.

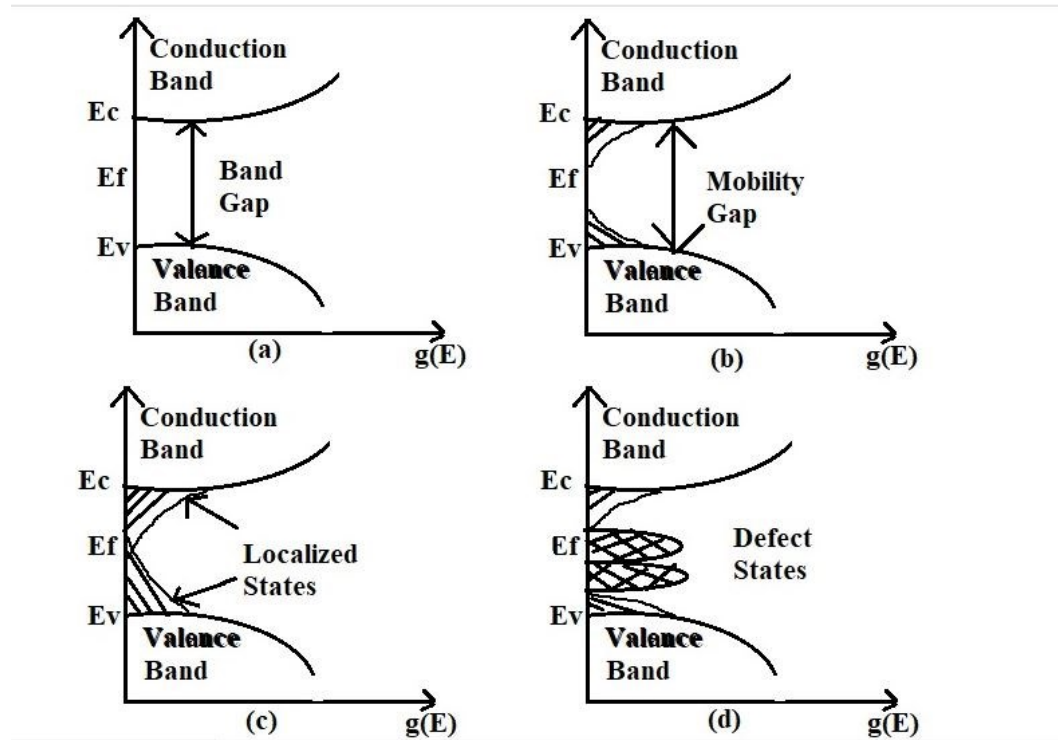


Fig 1.2 (a) Energy band diagram of crystalline semiconductor [7] (b) Energy band model proposed by Mott for amorphous semiconductor [8] (c) The CFO model for amorphous semiconductors [9] (d) Deep localized states proposed by Marshall and Owen [10].

In Figure 1.2 (a) the band model for crystalline semiconductor is presented. Due to periodic atomic arrangement, it has sharp band edge and defined forbidden band gap [7]. Figure 1.2 (b) represents the band model for amorphous semiconductor proposed by N.F. Mott in 1960s. Based on the two features of crystalline semiconductor, he developed the band model for amorphous semiconductor. One of the features is that the extended Bloch wave functions describe that the

individual atom inside the crystal lattice possess long range order in amplitude and phase. And the other one is that the well-defined energy gap known as forbidden energy gap separates the valence and conduction bands. Based on these two features, Mott assumed that all amorphous semiconductors have common characteristics including short-range order in the Bloch wave functions for electrons in their phases and long-range order in their amplitudes resulting in the localized states encroaching the bandgap [8].

Figure 2.2 (c) represents the Cohen, Fritzsche and Ovshinski (CFO) model for amorphous semiconductors which is an extension model of N.F. Mott. In this model the localized states are continuous through the bandgap and overlap in the region of fermi level [9]. Figure 2.2 (d) represents the Marshal and Owen model where the concentration of defect states in band gap are assumed to be high. There are two defect states appearing above and below the Fermi level. These two defect states act as donor and acceptor like states, and they significantly influence the electrical and optical properties of the amorphous materials [10].

1.3 Research motivation

1.3.1 Conventional Einstein Relation (CER)

A carrier in a uniform media can jump to any neighbouring site in any direction due to the thermal energy. The probability of this jump may depend on energy, distance, transfer mechanism etc. This random direction motion is called diffusion [12].

Alternatively, when electric field is applied to the sample, it causes an energy difference between the terminals and creates a preferred direction of charge flow. The proportionality constant between this charge flow and the electric field is called mobility provided that the drift velocity is lower than the thermal velocity. The diffusion coefficient and mobility are closely related and the relation between them is called the Einstein relation (ER) [12]. For avoidance of doubt, this term will be considered as the conventional Einstein relation.

$$\frac{D}{\mu} = \frac{kT}{e} \quad (1.1)$$

Here, D is diffusion coefficient, μ is the mobility, k is the Boltzmann constant, T is the temperature and e is the elementary charge.

1.3.2 Deviation from Conventional Einstein Relation (CER)

Through the time of flight (TOF) experiment, Richert *et al.* [13] and Borsenberger *et al.* [15] demonstrated that crystalline semiconductor obeys ER and follows $\frac{D}{\mu} = \frac{kT}{e}$ equation. However, in amorphous semiconductor, the presence of multiple traps (due to random orientation in atomic structure) in mobility gap raises disorder and the signals from TOF experiment often give dispersive transport indicating that the carriers cannot relax to dynamic equilibrium within the transit time. In other cases, the signals from TOF experiment shows a plateau region (gaussian profile) which is non-dispersive [13]. This indicates that disorder semiconductors do not follow the ER, which was later confirmed by Richert *et al.* [13]. Generally, the deviation of ER involves the assumption of media being isotropic and electric field being low enough to maintain linear response [13].

Compared to crystalline materials, the charge transport properties of amorphous materials are more complex to model and represent mathematically due to their disordered nature. With the use of quantum mechanics, crystalline materials can be easily expressed since their long-range order greatly simplifies the mathematical models involved. The study of amorphous materials then, relies heavily on empirical measurements of the physical and electronic properties of interest. The Time-of-Flight (TOF) transient photoconductivity experiment provides an excellent means to study the charge transport properties of low mobility solids such as amorphous materials. The Time-of-Flight (TOF) transient photoconductivity experiment consists of measuring the transient response that occurs due to the drift of injected charge carriers across a high resistivity solid.

Koughia et. al. investigated the distribution of localized states (DOS) in stabilized a-Se by comparing the measured and calculated electron time-of-flight (TOF) transient photocurrents. The theoretical analysis of multiple-trapping transport has been performed by the discretization of a continuous DOS and the use of Laplace transform formalism [16]. Kasap et. al. examine electron and hole transport in pure and stabilized amorphous selenium and attempt to construct a DOS distribution in the mobility gap based on time-of-flight (TOF) transient photoconductivity measurements [17]. Benkhedir et. al. also use transient photocurrent measurements on evaporated a-Se layers to specify the presence of two sets of discrete traps in the band tail region [18].

The charge carrier statistics and transport in disordered semiconductors do not follow the conventional equations for non-degenerate semiconductors because of existence of the mobility gap states. For example, the effective drift mobility is highly controlled by the states near the

mobility edges [19]. The ratio of the diffusion coefficient and drift mobility in crystalline semiconductor under a wide range of carrier concentration can conveniently be calculated by the Einstein relation. The density of states (DOS) in the mobility gap in amorphous/disordered semiconductors can change ER. It has been noted that the ratio of the diffusion coefficient and drift mobility is larger than the ER of k_bT/e even at the presence of smaller population than the degenerate limit [20] [21] in amorphous semiconductors.

Nguyen and O’Leary [20] analyzed the Einstein relation in disordered semiconductors with exponentially decaying tail states and square-root distribution of extended band states under thermal equilibrium. More recently, Çopuroglu and Mehmetoglu [22] determined an approximate analytical expression for Einstein relation based on the general frame work developed by Nguyen and O’Leary [20], Wei *et al.* [21] analyzed the Einstein relation in organic semiconductors having one or more Gaussian distributions of density of states (DOS) under thermal equilibrium. However, there exists a combination of exponentially decaying tail states and one or more Gaussian distributions of defect states (away from the mobility edges) in the mobility gap in some disordered semiconductors (e.g., amorphous selenium) [23] which was not considered before. Amorphous selenium-based X-ray detectors are widely used in diagnostic medical imaging especially in mammograph [24]. The performance of the detector highly depends on the charge carrier transport of the photoconductor [25].

1.4 Research Objectives

In this thesis work, the generalised Einstein relation (GER), namely, the diffusivity-mobility ratio, in disordered semiconductors with square-root distribution of band states, and exponential distributions of tail states and one or more Gaussian distributions of defect states near the mobility edges is analyzed. Furthermore, an analytical expression for the field stimulated diffusion coefficient under quasi-equilibrium condition for the same DOS distribution considering multiple trapping model is developed. The GER as a function of Fermi energy, electric field, and carrier concentration is also analysed. The model of GER is then applied to electrons and holes in a-Se. Finally, the field diffusion coefficient as a function of electric field and carrier concentration is analyzed.

1.5 Thesis Outline

The thesis work is organised in five chapters.

Chapter 2 focuses on a-Se, which is the primary subject matter of this thesis. The discussion in this chapter includes band structure, density of states, and application of a-Se. This chapter also includes carrier statistic in degenerate and nondegenerate semiconductors, which demonstrates that the Boltzmann approximation does not hold for degenerate semiconductors.

Chapter 3 explores theoretical aspects of charge carrier transport under multiple trapping at quasi thermal equilibrium. Further, the derivation of Einstein relation, charge transport for a-Se with

introduction of a new diffusion coefficient called field diffusion coefficient are included in this chapter.

The results and discussions of the thesis work are described in chapter 4. This includes the effects of different density of states parameters of a-Se on GER and the dependence of the field-diffusion coefficient on electric field and carrier concentration.

Chapter 5 presents the conclusion of this thesis work. This includes the overall conclusion of the work, its contribution, and future research prospects.

Chapter 2: Amorphous Selenium

2.1 Introduction

The subject matter of this thesis revolves around electrical properties of a-Se at degenerate limit. This chapter explains relevant theoretical premises including carrier statistics in non-degenerate and degenerate semiconductors at thermal equilibrium and DOS of a-Se.

2.2 Carrier Statistics in Non-degenerate and Degenerate Semiconductors in Thermal Equilibrium

A semiconductor sample is considered to have thermal equilibrium when there is no external force applied to it such as voltage, electric field, temperature gradient etc. The electrical properties of semiconductors can be changed by adding impurities called dopant atoms. Adding dopant atoms changes the distribution of electrons among the conduction and valance band states, causing the Fermi level to become a function of the type and concentration of dopant atoms.

The electron concentration per unit energy per unit volume in the conduction band is [2],

$$n(E) = g_c(E) f_F(E) \tag{2.1}$$

Here, $n(E)$ is the concentration of electrons, $g_c(E)$ is the density of states. The unit of $n(E)$ and $g_c(E)$ is $\text{cm}^{-3}\text{eV}^{-1}$. $f_F(E)$ is the probability that a state is occupied by an electron called Fermi-Dirac probability function.

The total electron concentration per unit volume in the conduction band is then found by integrating Equation (2.1) over the entire conduction-band energy [2],

$$n_0 = \int g_c(E) f_F(E) dE \quad (2.2)$$

For non-degenerate semiconductor, it is assumed that the Fermi level is within the forbidden energy band gap and Fermi-Dirac probability function is reduced to Boltzmann approximation [2].

$$f_F(E) = \frac{1}{1 + \exp\left(\frac{E - E_F}{kT}\right)} \quad (2.3)$$

$$f_F(E) \approx \exp\left[\frac{-(E - E_F)}{kT}\right] \quad (2.4)$$

Applying the Boltzmann approximation to Equation (2.2), the thermal-equilibrium density of electrons in the conduction band is found from [2],

$$n_0 = \int_{E_c}^{\infty} \frac{4\pi(2m_n)^{\frac{3}{2}}}{h^3} (\sqrt{E - E_c}) \exp\left[\frac{-(E - E_F)}{kT}\right] dE \quad (2.5)$$

$$n_0 = 2 \left(\frac{2\pi m_n kT}{h^2}\right)^{\frac{3}{2}} \exp\left[\frac{-(E_c - E_F)}{kT}\right] \quad (2.6)$$

$$n_0 = N_c \exp\left[\frac{-(E_c - E_F)}{kT}\right] \quad (2.7)$$

Here,

$$N_c = 2 \left(\frac{2\pi m_n^* kT}{h^2} \right)^{\frac{3}{2}} \quad (2.8)$$

The parameter N_c is called the effective density of states at conduction band, h is the Planck constant, m_n^* is called effective mass. For degenerate semiconductor, Boltzmann approximation does not hold. By using Fermi-Dirac probability function the thermal equilibrium electron concentration is written from equation (2.2) as [2],

$$n_0 = \frac{4\pi}{h^3} (2m_n^*)^{\frac{3}{2}} \int_{E_c}^{\infty} \frac{\sqrt{E - E_c}}{1 + \exp\left(\frac{E - E_F}{kT}\right)} dE \quad (2.9)$$

$$n_0 = 4\pi \left(\frac{2m_n^* kT}{h^2} \right)^{\frac{3}{2}} \int_0^{\infty} \frac{\sqrt{z}}{1 + \exp(z - n)} dz \quad (2.10)$$

Where,

$$z = \frac{E - E_c}{kT} \text{ and } n = \frac{E_F - E_c}{kT} \quad (2.11)$$

Introducing gamma function,

$$n_0 = \frac{4\pi (2m_n^* kT)^{\frac{3}{2}}}{h^3} \frac{\sqrt{\pi}}{2} \frac{1}{\Gamma\left(\frac{1}{2} + 1\right)} \int_0^{\infty} \frac{\sqrt{z}}{1 + \exp(z - n)} dz \quad (2.12)$$

Here,

$$\Gamma\left(\frac{1}{2}\right) = \sqrt{\pi}$$
$$\Gamma(x+1) = x\Gamma(x)$$

Therefore, electron concentration at degenerate limit [2],

$$n_0 = N_c F_{\frac{1}{2}}(n) \quad (2.13)$$

Here Fermi-Dirac integral,

$$F_j(n) = \frac{1}{\Gamma(j+1)} \int_0^\infty \frac{\sqrt{z}}{1 + \exp(z-n)} dz \quad (2.14)$$

2.3 Amorphous Selenium

The name “Selenium” originates from the Greek word for moon: “Selene”. Selenium was discovered by Jons Jacob Berzelius in 1817. The Amorphous Selenium (a-Se) has low melting temperature and high vapour pressure which makes it easy to deposit as thick and uniform layers over a large area. a-Se offers great advantages over other chalcogenide glasses. Firstly, both the hole and electron can drift throughout the material resulting in increasing overall photoconductivity. Secondly, the electronic properties of a-Se are highly responsive to impurities (even in ppm range). Hence, by adding small amount of impurities the whole material can change into either p-type or n-type.

2.3.1 Uses of Amorphous Selenium

Photoconductor was first discovered by W. Smith in 1873 [26], when he was using rods of selenium as resistors to test sub-marine telepathic cables. He discovered that the resistance of these rods depends on whether the resistor is illuminated or not. Selenium solar cell was first reported in 1883. Between 1920s and 1950s, selenium solar cells were available before silicon solar cells were produced. Electrical rectifiers used the crystalline selenium from the 1930s to the 1960s.

Firstly, the low melting point and high vapour pressure allows for a thick layer of a-Se being deposited. While the atomic number (34) for a-Se is not as high as some of the other X-ray photoconductors, it can nonetheless absorb X-rays, especially in the mammographic range [28].

Secondly, a-Se can be readily coated by conventional vacuum deposition over a large area with good uniformity up to thicknesses of 1000 μm . This trait is particularly useful, since X-rays cannot practically be focused and requires image detectors to be larger than the body parts to be imaged [28].

Thirdly, both holes and electrons are mobile in a-Se, which is a distinct advantage because X-rays are absorbed throughout the a-Se layer. Thus, both the electrons and holes generated by the absorption of an X-ray photon can drift and be collected [28].

Fourthly, unlike many other amorphous solids, charge transport in a-Se over the time scale of interest at room temperature is moderately dispersive for both holes and electrons. Hence, both

hole and electron transport can be readily described by a set of shallow traps that control the drift mobility and a distribution of deep traps with well-defined trapping times or lifetimes. And finally, the dark current in a-Se photoconductors tends to be relatively small compared with many other competing photoconductors [28].

2.4 Density of States of a-Se

For Amorphous selenium, there are two prominent sets of traps called shallow and deep trap in the mobility gap. Shallow traps are close to mobility edges and hence are usually considered for charge transport equation. The release time from deep trap is longer than the time scale of interest and thus the deep traps determine carrier lifetime. In Figure 2.1 there is a detailed illustration of localized density-of-states distribution in a-Se [23].

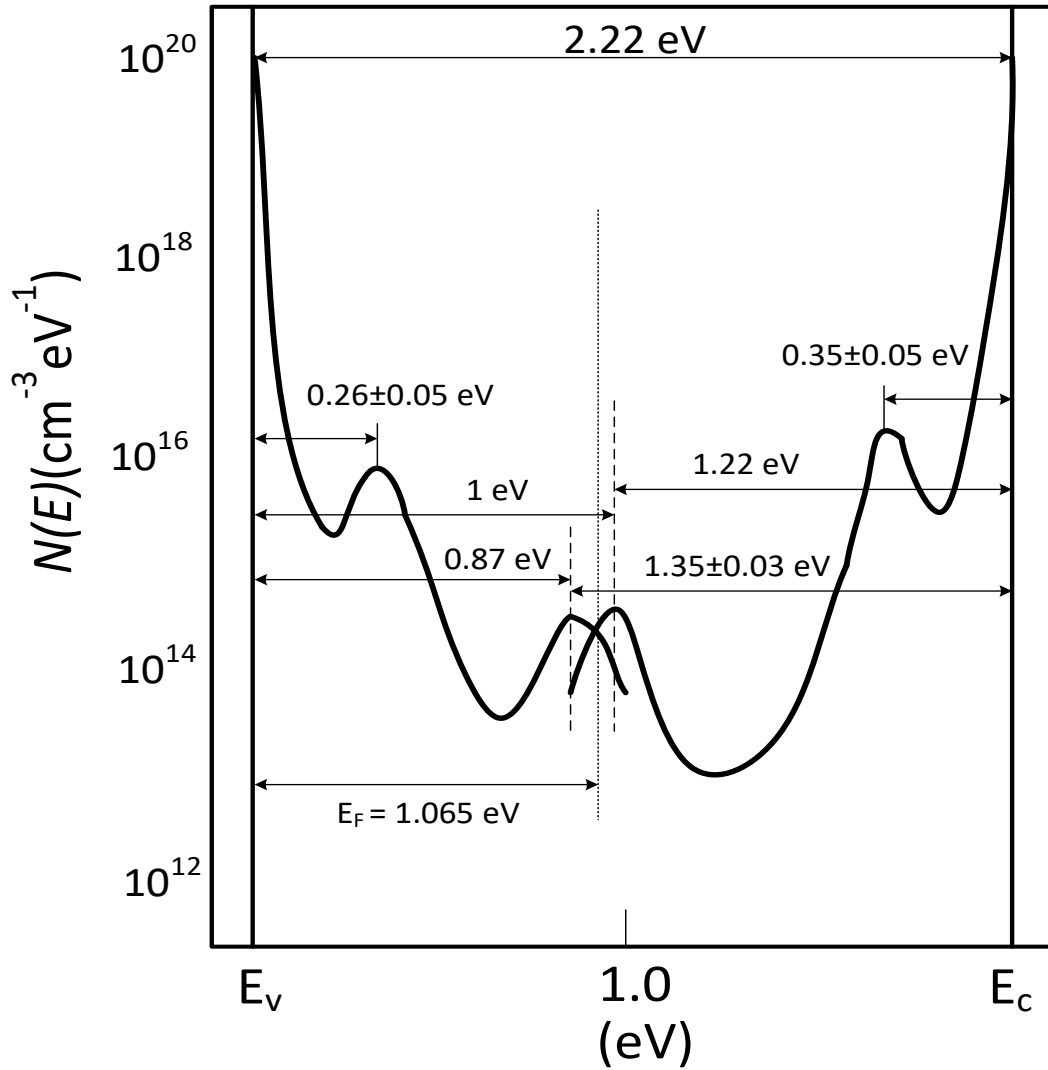


Fig 2.1: The localized density-of-states distribution in a-Se according to the Abkowiz model [23].

There have been significant prior studies on electronic properties of a-Se since M. Abkowiz has proposed a complete DOS for a-Se [23] which showed distinct peaks in the tail (or localized gap) states that has later been validated by others [16], [17], [18]. A general consensus on the DOS

distribution near the mobility edges is that it is not a single exponentially decaying function (as opposed to a-Si:H) but exhibits certain peaks whose exact positions are still controversial. Though there are controversies on the magnitude and position of the peak, the density of states function for the shallow traps (g_s) near conduction (or valence) band can be approximated as the sum of the exponential tail and one or more Gaussian peaks [29],

$$g_s(E) = g_c \exp[-(E_c - E)/kT_0] + \sum_{i=1}^N N_{mi} \exp\left\{-\frac{(E - E_{mi})^2}{\Delta E_{mi}^2}\right\}, \quad (2.15)$$

Where, T_0 is the characteristic temperature, g_c is the density of states at the conduction band edge, E_c is the conduction band mobility edge, N_{mi} is the peak value of shallow traps at $(E_c - E) = E_{mi}$ and $i = 1, 2, \dots, N$ (N is determined by the number of shallow Gaussian peaks in DOS), ΔE_{mi} is the width of the Gaussian peak. Note that the shallow trapping states affect the effective drift mobility whereas the deep trapping states are responsible for average carrier lifetime [30]. The variations on the values of DOS parameters reported in different publications in literature for shallow traps for electrons and holes are summarized in Table I and II, respectively.

Table I: DOS below conduction-band mobility edge, E_c in the mobility gap. Note that E_m is measured from E_c .

Ref.	Exponential Tail	Gaussian peak 1 (Below E_c)	Gaussian Peak 2 (Below E_c)
M.Abkowitz [23]	$g_c = 10^{20} \text{ eV}^{-1}\text{cm}^{-3}$	$E_m = 0.33 - 0.37 \text{ eV}$ $N_m = 10^{16} \text{ eV}^{-1}\text{cm}^{-3}$	
Koughia <i>et al.</i> [16]	$g_c = 2 \times 10^{21} \text{ eV}^{-1}\text{cm}^{-3}$	$E_m = 0.3 - 0.35 \text{ eV}$ $\Delta E_m = 0.035 \text{ eV}$ $N_m = 2.4 \times 10^{16} \text{ eV}^{-1}\text{cm}^{-3}$	$E_m = 0.5 \text{ eV}$ $\Delta E_m = 0.04 \text{ eV}$ $N_m = 5.6 \times 10^{13} \text{ eV}^{-1}\text{cm}^{-3}$
Kasap <i>et al.</i> [17]	$g_c = 2 \times 10^{21} \text{ eV}^{-1}\text{cm}^{-3}$	$E_m = 0.27 - 0.33 \text{ eV}$ $\Delta E_m = 0.03 - 0.04 \text{ eV}$ $N_m = 10^{17} - 10^{18} \text{ eV}^{-1}\text{cm}^{-3}$	$E_m = 0.38 - 0.48 \text{ eV}$ $\Delta E_m = 0.04 - 0.06 \text{ eV}$ $N_m = 5 \times 10^{13} -$ $5 \times 10^{15} \text{ eV}^{-1}\text{cm}^{-3}$
Benkhedir <i>et al.</i> , [18]		$E_m = 0.26 - 0.3 \text{ eV}$	$E_m = 0.53 \text{ eV}$

Table II: DOS above valence-band mobility edge, E_v in the mobility gap

Ref.	Exponential Tail	Gaussian peak 1 (Above E_v)	Gaussian peak 2 (Above E_v)
M.Abkowitz [23]	$g_v = 10^{20} \text{ eV}^{-1} \text{ cm}^{-3}$	$E_m = 0.24 - 0.28 \text{ eV}$ $N_m = 10^{16} \text{ eV}^{-1} \text{ cm}^{-3}$	
Kasap <i>et al.</i> [17]	$g_v = 2 \times 10^{21} \text{ eV}^{-1} \text{ cm}^{-3}$		
Benkhedir <i>et al.</i> [18]		$E_m = 0.18 - 0.22 \text{ eV}$	$E_m = 0.36 - 0.4 \text{ eV}$

Considering a square root distribution for the extended states, the complete DOS near conduction band edge can be written according to Nguyen and O'Leary[20],

$$\begin{aligned}
 g(E) &= \left[g_c \sqrt{\frac{2}{\gamma_c}} \left(\sqrt{E - E_c + \frac{\gamma_c}{2}} \right) \right]; E \geq E_c \\
 &= \left[g_c \exp\left(\frac{-(E_c - E)}{\gamma_c}\right) + \sum_{i=1}^N N_{mi} \exp\left(\frac{-(E - E_{mi})^2}{\Delta E_{mi}^2}\right) \right]; E < E_c
 \end{aligned} \tag{2.16}$$

Here $\gamma_c = kT_0$, represents the decay rate of the exponential tail states in mobility gap. The valence-band DOS distribution is similar to the conduction band DOS distribution and the relation for holes, D_h/μ_h , can also be derived using the similar technique.

Chapter 3: Modeling of Diffusion Coefficient in Disordered Semiconductors

3.1 Introduction

This chapter demonstrates charge carrier transport under multiple trapping in mobility gap through a mathematical description. This chapter also derives a diffusion coefficient from GER at low electric field as well as a diffusion coefficient from charge carrier transport under multiple trapping at high electric field. A mathematical expression of drift mobility at extended states is also presented in this chapter.

3.2 Charge Carrier Transport Under Multiple Trapping

The diffusion coefficient determined from Einstein relation in amorphous semiconductors is valid at quasi-equilibrium transport when the electric field is very low [31]. Under applied field, charge carriers undergo many trapping-detrapping events in the energy distributed mobility gap states during their travel. The statistical variations of the trapping and release times create a considerable spreading of signal. Thus, the actual diffusion coefficient appears to be much larger than it should be from the known Einstein relation [31] [32]. The additional diffusion coefficient is known as the field stimulated diffusion. Rudenko and Arkhipov [32] developed a formulation for field-diffusion coefficient (FDC) under quasi-equilibrium condition considering multiple trapping model. However, their formulation is valid for small signal condition and thus it is independent of carrier concentration. Later, Li *et al.* [31] evaluated this diffusion coefficient for

organic semiconductors where the DOS consists of a single Gaussian peak only and considering carrier hopping transport. However, the multiple trapping model (i.e., the extended states transport with carriers trapped and released from the shallow trapping states) is more appropriate to describe the charge carrier transport in amorphous semiconductors at room temperature [33]. Nikitenko and Kudrov [33] described field diffusion coefficient (FDC) considering multiple trapping model, which is applicable to organic semiconductors having a DOS distribution consists of a single Gaussian peak only.

The multiple trapping model (i.e., the extended states transport with carriers trapped and released from the shallow trapping states) can successfully describe the charge carrier transport in amorphous semiconductors [34]. In multiple trapping model, the continuity equation for electrons including carrier drift and diffusion under uniform electric field F can be written as,

$$\frac{\partial n(x,t)}{\partial t} - \mu_{0e} F \frac{\partial n_c(x,t)}{\partial x} - D_{0e} \frac{\partial^2 n_c(x,t)}{\partial x^2} = 0 \quad (3.1)$$

Where x is the space co-ordinate, t is the time, n is the total electron concentration in DOS considering electrons in the extended and shallow states, n_c is the electron concentration in the extended states (i.e., the quasi-free electron concentration), μ_{0e} and D_{0e} are the drift mobility and diffusion coefficient of electrons at the extended states. Note that the states above the conduction band edge (E_c) are termed as the extended states and the states below but close to E_c are called the shallow states. The carrier release phenomenon from a shallow trap is much faster, and the carrier trapping is balanced by the carrier release process. Therefore, the kinetic equation for the

trapped electron concentration (n_t) at energy E from the conduction band edge is

$$\frac{dn_t(E, x, t)}{dt} = C_t(E) [g(E) - n_t(E, x, t)] n_c(x, t) - \nu n_t(E, x, t) \exp[-(E_c - E)/k_b T] \quad (3.2)$$

Where,

$$n(x, t) = n_c(x, t) + n_t(x, t) \quad (3.3)$$

And

$$n_t(x, t) = \int_{-\infty}^{E_c} n_t(E, x, t) dE \quad (3.4)$$

Here E_c is the energy at the conduction band mobility edge, C_t is the capture coefficient of free electrons, $g(E)$ is the density of states of a-Se at energy E in the mid gap, n_c is the quasi-free electron concentration, and ν is the attempt-to-escape frequency. The relation between ν and C_t can be determined by the principle of detailed balance, which gives $\nu = N_c C_t = (g_c k T) C_t$, where g_c is the density of states at the conduction band edge and $(g_c k T)$ is approximately the effective density of states N_c at the conduction band. If ν is independent of energy, then C_t is also independent of energy. For simplicity, C_t is assumed to be independent of energy [32].

A equilibrium transport is reached when the concentration of free electrons n_c is in equilibrium with the trapped concentration n_t . Under this equilibrium transport (i.e., at steady state), the time derivative in equation (3.2) is zero and thus,

$$C_t(E) [g(E) - n_t(E, x, t)] n_c(x, t) = \nu n_t(E, x, t) \exp\left[\frac{-(E_c - E)}{k_b T}\right] \quad (3.5)$$

From the relation of ν (attempt-to-escape frequency) and C_t (capture coefficient of free electrons) and considering C_t is to be independent of energy equation (3.5) can be written as

$$n_t(E, x, t) = \frac{g(E)n_c(x, t)}{n_c(x, t) + N_c \exp\left(\frac{-(E_c - E)}{k_b T}\right)} \quad (3.6)$$

Substituting $n_t(E, x, t)$ from equation (3.6) into equation (3.4),

$$n_t(x, t) = n_c(x, t) \int_{-\infty}^{E_c} \frac{g(E)}{N_c \exp\left[-(E_c - E_{Fn})/k_b T\right] + N_c \exp\left[-(E_c - E)/k_b T\right]} dE \quad (3.7)$$

Where the quasi-Fermi level E_{Fn} is determined by the carrier concentration in the extended states as,

$$E_{Fn}(x, t) = E_c - k_b T \ln\left[N_c / n_c(x, t)\right] \quad (3.8)$$

So the total carrier concentration $n(x, t)$ can be written as,

$$n(x, t) = n_c(x, t) + n_c(x, t) \int \frac{g(E)}{N_c \exp\left[\frac{-(E_c - E_{Fn})}{k_b T}\right] + N_c \exp\left[\frac{-(E_c - E)}{k_b T}\right]} dE \quad (3.9)$$

Under non-degenerate limit, the first term in the denominator of equation (3.7) is much smaller than the second term. In other words, neglecting the trap saturation effect (second term in

equation (3.2)). Under small signal, n_i in equation (3.7) is independent of extended state carrier concentration. Thus, the free carrier concentration from equation (3.9) can be expressed as [32],

$$n_c(x,t) = n_c(x,t) \left[1 + \int_{-\infty}^{E_c} \frac{g(E)}{N_c} \left(\exp \left[\frac{E_c - E}{k_b T} \right] \right) dE \right] \quad (3.10)$$

Thus, the relation between free carrier concentration and total carrier concentration is expressed as,

$$n_c(x,t) = \left[\frac{\theta_e}{1 + \theta_e} \right] n(x,t) \quad (3.11)$$

Where,

$$\theta_e^{-1} = \int_{-\infty}^{E_c} \left[g(E) / N_c \right] \exp \left[(E_c - E) / k_b T \right] dE \quad (3.12)$$

Substituting n_c from equation (3.10) into equation (3.1) gives,

$$\frac{\partial n(x,t)}{\partial t} - \mu_e F \frac{\partial n(x,t)}{\partial x} - D_e \frac{\partial^2 n(x,t)}{\partial x^2} = 0 \quad (3.13)$$

Where,

$$\mu_e = \left[\frac{\theta_e}{1 + \theta_e} \right] \mu_{0e} \quad (3.14)$$

$$D_e = \left[\frac{\theta_e}{1 + \theta_e} \right] D_{0e} \quad (3.15)$$

The parameters μ_e and D_e are named as the effective drift mobility and diffusion coefficient of electrons [30].

3.3 Modeling Diffusion Coefficient from GER

The effective drift mobility in amorphous semiconductor is shallow-trapped controlled and thermally activated. The effective drift mobility is reduced by the trapping and release events, and, under quasi-equilibrium, the drift mobility is the multiplication of the extended state mobility and a factor for the trapping and release event.

The drift current density j_{dr} and diffusion current density j_d of electrons at x with an electric field $F(x)$ can be written as,

$$j_{dr} = en\mu_e F \quad (3.16)$$

$$j_d = eD_e \frac{dn}{dx} \quad (3.17)$$

where n is the total electron density considering electrons in the extended and shallow states, μ_e and D_e are the effective drift mobility and diffusion coefficient from equation (3.14) and (3.15) of electrons [30]. The electric field can be expressed as [35],

$$dV = -Fdx \quad (3.18)$$

At thermal equilibrium, the drift and diffusion currents are equal and flow in the opposite directions. Equating equations (3.16) & (3.17) and replacing the expression of F [35],

$$\frac{D_e}{\mu_e} = \frac{n}{\frac{dn}{dV}} \quad (3.19)$$

To make the derivation more formal the fact that a difference in potential between two points are defined as the difference between the quasi-Fermi-levels is assumed,

$$dV = edE_{Fn} \quad (3.20)$$

where E_{Fn} is the quasi-Fermi energy of electrons at position x .

Thus, the general form of Einstein relation (GER) which related the effective diffusion coefficient and drift mobility is given by [20] [22],

$$\frac{D_e}{\mu_e} = \frac{D_{0e}}{\mu_{0e}} = \frac{n}{e \frac{dn}{dE_{Fn}}} \quad (3.21)$$

Where E_{Fn} is the quasi-Fermi energy of electrons in eV . Equation (3.21) is widely used for determining Einstein relation in crystalline semiconductors. One can use the same form of Einstein relation in disordered semiconductors under thermal equilibrium provided that the small signal criteria are met when the trap saturation effect can be neglected.

The electron occupancy probability at energy E is determined by the Fermi-Dirac statistics and given by,

$$f(E, E_{Fn}) = \frac{1}{1 + \exp\left(\frac{E - E_{Fn}}{kT}\right)} \quad (3.22)$$

In the case of pure crystalline semiconductors within the non-degenerate limit, i.e., when the Fermi level is within the bandgap and not closer than $3kT$ to the band edges,

$$n(E_{Fn}) = N_c \exp\left(\frac{E_{Fn} - E_c}{kT}\right) \quad (3.23)$$

In this case,

$$\frac{dn}{dE_{Fn}} = \frac{n}{kT} \quad (3.24)$$

and equation (3.21) becomes,

$$\frac{D_e}{\mu_e} = \frac{kT}{e} \quad (3.25)$$

Equation (3.25) is the conventional Einstein relation (CER) in pure crystalline semiconductors under non-degenerate limit. For disordered or degenerate semiconductors, there is no simple analytical expression for n and the total electron concentration in DOS can be written as,

$$n(E_{Fn}) = \int_{-\infty}^{\infty} g(E) f(E, E_{Fn}) dE \quad (3.26)$$

Where $g(E)$ is the density of states. Once $g(E)$ is known, n can be determined and equation (3.21) becomes,

$$\frac{D_e}{\mu_e} = \frac{kT}{e} \frac{\int_{-\infty}^{\infty} g(E) \left[1 + \exp\left(\frac{E - E_{Fn}}{kT}\right)\right]^{-1} dE}{\int_{-\infty}^{\infty} g(E) \exp\left(\frac{E - E_{Fn}}{kT}\right) \left[1 + \exp\left(\frac{E - E_{Fn}}{kT}\right)\right]^{-2} dE} \quad (3.27)$$

Note that the difference between two integrals of equation (3.26) depends on mobility gap states and Fermi energy.

3.4 Developing Field Diffusion Coefficient Under Quasi-Equilibrium Transport

The transport of excess carriers in disordered semiconductors with a wide spectrum of localized states can not be described by the instantaneous establishment of equilibrium transport described above. Rudenko and Arkhipov [32] described the quasi-equilibrium transport (i.e., relaxing the steady-state solution of equation (3.2)) behavior by assuming that the third term of equation (3.2) is small compared to the first term. That means, the release event is slower than the trapping event. However, their formulations are valid under small signal case since they neglected trap saturation effect in equation (3.2). Nikitenko and Kudrov [33] extended the model by incorporating trap saturation effect. The approximate continuity equation under quasi-equilibrium transport was proposed as [32] [33],

From equation (3.2),

$$n_t(E,x,t) = n_t^o(E,x,t) - \frac{\frac{dn_t(E,x,t)}{dt}}{C_t(E) \left[n_c(x,t) + N_c \exp \left[\frac{-(E_c - E)}{k_b T} \right] \right]} \quad (3.28)$$

Where,

$$n_t^0(E,x,t) = \frac{g(E) n_c(x,t)}{n_c(x,t) + N_c \exp\left[\frac{-(E_c - E)}{k_b T}\right]} \quad (3.29)$$

Integrating equation (3.27) with respect to energy, using equation (3.8) ,

$$\int_{-\infty}^{E_c} n_t^0(E,x,t) dE = n_c(x,t) \int_{-\infty}^{E_c} \frac{g(E)}{N_c \exp\left[\frac{-(E_c - E_{Fn})}{k_b T}\right] + N_c \exp\left[\frac{-(E_c - E)}{k_b T}\right]} dE \quad (3.30)$$

$$\int_{-\infty}^{E_c} n_t^0(E,x,t) dE = n_c(x,t) \frac{1}{\theta_{el}} \quad (3.31)$$

$$\theta_{el}^{-1} = \int_{-\infty}^{E_c} \frac{g(E) \exp\left[\frac{(E_c - E)}{k_b T}\right]}{N_c \left[1 + \exp\left(\frac{E_{Fn} - E}{k_b T}\right)\right]} dE \quad (3.32)$$

Considering trap saturation effect, equation (3.11), (3.14), (3.15) become,

$$n_c(x,t) = \left[\frac{\theta_{el}}{1 + \theta_{el}} \right] n(x,t) \quad (3.33)$$

$$\mu_e = \left[\frac{\theta_{el}}{1 + \theta_{el}} \right] \mu_{0e} \quad (3.34)$$

$$D_e = \left[\frac{\theta_{el}}{1 + \theta_{el}} \right] D_{0e} \quad (3.35)$$

From equation (3.6),

$$n_t(E,x,t) = \frac{g(E) n_c(x,t)}{n_c(x,t) + N_c \exp\left[\frac{-(E_c - E)}{k_b T}\right]} \quad (3.36)$$

Differentiating equation (3.36) with respect to time,

$$\frac{d}{dt} n_t(E,x,t) = \frac{g(E) N_c \exp\left[\frac{-(E_c - E)}{k_b T}\right] \frac{d}{dt} n_c(x,t)}{\left[n_c(x,t) + N_c \exp\left[\frac{-(E_c - E)}{k_b T}\right]\right]^2} \quad (3.37)$$

From equation (3.26),

$$n_t(E,x,t) = n_t^0(E,x,t) - \frac{g(E) N_c \exp\left[\frac{-(E_c - E)}{k_b T}\right] \frac{d}{dt} n_c(x,t)}{C_t(E) \left[n_c(x,t) + N_c \exp\left[\frac{-(E_c - E)}{k_b T}\right]\right]^3} \quad (3.38)$$

Integrating equation (3.31) with respect to energy,

$$\int_{-\infty}^E n_t(E,x,t) dE = \int_{-\infty}^E n_t^0(E,x,t) dE - \int_{-\infty}^E \frac{g(E) N_c \exp\left[\frac{-(E_c - E)}{k_b T}\right] \frac{d}{dt} n_c(x,t)}{C_t(E) \left[n_c(x,t) + N_c \exp\left[\frac{-(E_c - E)}{k_b T}\right]\right]^3} dE \quad (3.39)$$

Applying equation (3.3), (3.4), (3.31), (3.33), (3.37) into equation (3.39),

$$n_c(x,t) = \frac{\theta_{el}}{1 + \theta_{el}} n(x,t) + \frac{\theta_{el}^2}{(1 + \theta_{el})^2} \frac{1}{\omega} \frac{dn(x,t)}{dt} \quad (3.40)$$

Where,

$$\frac{1}{\omega} = \frac{1}{v} \int_{-\infty}^{E_c} \frac{1}{N_c} \frac{g(E) \exp\left[\frac{2(E_c - E)}{k_b T}\right]}{\left[1 + \exp\left[\frac{(E_{Fn} - E)}{k_b T}\right]\right]^3} dE \quad (3.41)$$

Substituting equation (3.13) into (3.40),

$$n_c(x,t) = \frac{\theta_{el}}{1 + \theta_{el}} n(x,t) + \frac{\theta_{el}^2}{(1 + \theta_{el})^2} \frac{1}{\omega} \left[\mu_e F \frac{\partial n(x,t)}{\partial x} + D_e \frac{\partial^2 n(x,t)}{\partial x^2} \right] \quad (3.42)$$

From equation (3.1),

$$\begin{aligned} & \frac{\partial n(x,t)}{\partial t} - \mu_{oe} F \left[\frac{\partial}{\partial x} \left[\frac{\theta_{el}}{1 + \theta_{el}} n(x,t) + \frac{\theta_{el}^2}{(1 + \theta_{el})^2} \frac{1}{\omega} \left[\mu_e F \frac{\partial n(x,t)}{\partial x} + D_e \frac{\partial^2 n(x,t)}{\partial x^2} \right] \right] \right] \\ & - D_{oe} \left[\frac{\partial^2}{\partial x^2} \left[\frac{\theta_{el}}{1 + \theta_{el}} n(x,t) + \frac{\theta_{el}^2}{(1 + \theta_{el})^2} \frac{1}{\omega} \left[\mu_e F \frac{\partial n(x,t)}{\partial x} + D_e \frac{\partial^2 n(x,t)}{\partial x^2} \right] \right] \right] = 0 \end{aligned} \quad (3.43)$$

Ignoring higher order and applying (3.34) and (3.35),

$$\frac{\partial n(x,t)}{\partial t} - \mu_e F \frac{\partial n(x,t)}{\partial x} - \left[(\mu_e F)^2 \frac{\theta_{el}}{1 + \theta_{el}} \frac{1}{\omega} + D_e \right] \frac{\partial^2 n(x,t)}{\partial x^2} = 0 \quad (3.44)$$

$$\frac{\partial n(x,t)}{\partial t} - \mu_e F \frac{\partial n(x,t)}{\partial x} - (D_e + D_{fe}) \frac{\partial^2 n(x,t)}{\partial x^2} = 0 \quad (3.45)$$

Where,

$$D_{fe} = \left(\frac{\theta_{el}}{1 + \theta_{el}} \right)^3 \frac{F^2 \mu_{0e}^2}{\omega_e} \quad (3.46)$$

The term D_{fe} is named as the field diffusion coefficient, which is the addition term as compared to the thermal equilibrium case in equation (3.13). The field diffusion coefficient becomes carrier concentration dependent because of the second term in the denominator of equation (3.41), which arises by considering the trap saturation effect (second term in equation 3.2). Otherwise, D_{fe} is simply proportional to the square of electric field. For small signal and shallow trap levels $E > E_{Fn}$, the second term in the denominator of equation (3.41) is much smaller than one and can be neglected, which is the formulation of Rudenko and Arkhipov [32]. Therefore, the field diffusion coefficient is the maximum at small signal, decreases monotonously with increasing the carrier concentration and becomes negligibly small at very high carrier concentrations.

For the DOS profile in equation (3.2) and under small signal case, one can get analytical expressions for θ_e^{-1} and $\omega_{e,\max}^{-1}$ as [19],

$$\theta_e^{-1} \approx \left(\frac{T}{T_0} - 1 \right)^{-1} + \sum_{i=1}^N \left(\frac{\sqrt{\pi} \Delta E_{mi} N_{mi}}{kTg_c} \right) \exp \left\{ \left(\frac{\Delta E_{mi}}{2kT} \right)^2 + E_{mi} / k_b T \right\} \quad (3.47)$$

And,

$$\omega_{e,\max}^{-1} \approx \nu^{-1} \left\{ \left(\frac{T}{T_0} - 2 \right)^{-1} + \sum_{i=1}^N \left(\frac{\sqrt{\pi} \Delta E_{mi} N_{mi}}{kTg_c} \right) \exp \left[\left(\frac{\Delta E_{mi}}{kT} \right)^2 + 2E_{mi} / k_b T \right] \right\} \quad (3.48)$$

Thus, the maximum value of field diffusion coefficient is,

$$D_{fe,\max} \approx \left(\frac{\theta_e}{1 + \theta_e} \right)^3 F^2 \mu_{0e}^2 \omega_{e,\max}^{-1} \quad (3.49)$$

3.5 Effective Drift mobility for a-Se at High Electric Field

The theoretical model is applied to a-Se to find the effects of various parameters on the diffusion coefficient as a function of carrier concentration. The low-field extended state mobilities of electrons and holes in a-Se are found to be ~ 1 and $2.6 \text{ cm}^2/\text{Vs}$, respectively [36]. The effective drift mobility of both holes and electrons in a-Se increases with increasing temperature and applied electric field [37]. The effective drift mobilities of electrons and holes at room temperature and up to the moderate field ($F \leq 10 \text{ V}/\mu\text{m}$) are in the range $0.003\text{--}0.006$ and $0.12\text{--}0.14 \text{ cm}^2/\text{Vs}$, respectively [38]. The effective drift mobility of holes and electrons in a-Se at high electric fields increases with increasing field and reaches a saturation value at a field higher than $100 \text{ V}/\mu\text{m}$ [39]. For convenience, the empirical relations for the effective hole and electron mobilities in a-Se at high electric field ($F > 10 \text{ V}/\mu\text{m}$) and at room temperature are obtained by fitting the experimental results [37] [38] which are [36],

$$\mu_h(F) \approx 0.127 + \frac{0.745}{1 + \exp[-(F - 48)/11.5]} \quad (3.50)$$

$$\mu_e(F) \approx 0.005 + \frac{0.13}{1 + \exp[-(F - 110)/20]} \quad (3.51)$$

where F is the electric field in $\text{V}/\mu\text{m}$ and μ is the mobility in cm^2/Vs .

As mentioned earlier, the effects on holes are identical to electrons having the similar DOS parameters near the valence band. Therefore, for simplicity, only the effects of various DOS parameters on electron transport in Figures 4.1 to 4.4 is showed, considering only one Gaussian peak in mobility gap. As described in Tables I & II, the variations of parameters are observed as,

$g_c = 10^{20} - 2 \times 10^{21} \text{ cm}^{-3}\text{eV}^{-1}$, $E_m = 0.2 - 0.5 \text{ eV}$, $\Delta E_m = 0.03 \text{ to } 0.05 \text{ eV}$, and $N_m = 10^{13} - 10^{18} \text{ cm}^{-3}\text{eV}^{-1}$. The characteristic temperature in a-Se is found to be 275 K [36] and thus $\gamma_c = 0.02374 \text{ eV}$. Then, the Einstein relation for both electrons and holes using the values of different parameters from Tables I and II is presented.

3.6 Conclusion

The density of states of a-Se consists of defect states in mobility gap, which results in the diffusion coefficient of a-Se deviating from the ER and necessitating the development of diffusion coefficient from GER under quasi-equilibrium transport at low electric field. In high electric field, charge carriers of a-Se undergoes many trapping and detrapping events in the energy distributed mobility gap states during their travel. Hence, the actual diffusion coefficient appears to be much larger than it should be from the CER. The additional diffusional coefficient called field diffusion coefficient is developed from charge carrier statistics under multiple trapping.

Chapter 4: Result and discussion

4.1 Introduction

Chapter 3 has established the theoretical model of diffusion coefficient and field diffusion coefficient at low and high electric field respectively. In this chapter, those diffusion coefficients are graphically presented to validate ER for a-Se. The effects of the DOS parameters of a-Se on the Einstein relation as a function of carrier concentration is analysed in this chapter. Finally, an analysis of the field diffusion coefficient of electrons and holes in a-Se is also included in this chapter.

4.2 Diffusion coefficient from Einstein relation

The conventional Einstein relation in equation (3.25) provides the diffusion coefficient under thermal equilibrium. This thermal diffusion coefficient for a-Se is examined. The extended state electron concentration n_c is a function of the Fermi level, which is not influenced by the bandgap states. Therefore, the Fermi level or the extended state electron concentration n_c can be treated as the independent variable for examining the Einstein relation. Figure 4.3 shows the effect of N_m of a single Gaussian peak on the D_e/μ_e ratio as a function of extended state electron concentration n_c . The D_e/μ_e ratio is normalized with respect to kT/e . The following parameters are: $g_c = 4 \times 10^{20} \text{ cm}^{-3}\text{eV}^{-1}$, $E_m = 0.35 \text{ eV}$, $\Delta E_m = 0.05 \text{ eV}$ and $T = 295 \text{ K}$. The dotted line represents the normalized Einstein relation for no band gap states (i.e., a representation of pure crystalline case). The Einstein relation in pure crystalline semiconductors follows the traditional constant

value $D_e/\mu_e = kT/e$ up to the degenerate limit (i.e., $n \sim 10^{18} \text{ cm}^{-3}$). The difference between the dotted and solid line represents the effects of exponential tail states, which depends on γ_c . The effect of γ_c on Einstein relation has been described in detail in ref- [20] in this thesis work, it is considered a fixed value ($\gamma_c = 0.02374 \text{ eV}$) that is appropriate for a-Se. The ratio D_e/μ_e deviates and the deviation increases with increasing electron concentration. This ratio increases from 1.5 % to 5 % by increasing the electron concentration from 10^{10} to 10^{15} cm^{-3} . On the other hand, this deviation becomes very substantial with Gaussian peaks in DOS near the conduction band. The D_e/μ_e ratio shows a bump for one Gaussian peak in DOS with higher N_m leading to a higher peak and moving of the peak at a higher electron concentration. After the respective peaks, all curves for the D_e/μ_e ratio converge towards the degenerate case at very high electron concentration, which can be explained by the fact that the electron concentration in deep degenerate case is determined by the extended band states rather than the localized gap states. The effect of the width (ΔE_m) of Gaussian peak in DOS on the D_e/μ_e ratio is similar to the magnitude N_m (Figure 4.1). On the other hand, the effect of g_c on the D_e/μ_e ratio is opposite to that of N_m (Figure 4.2).

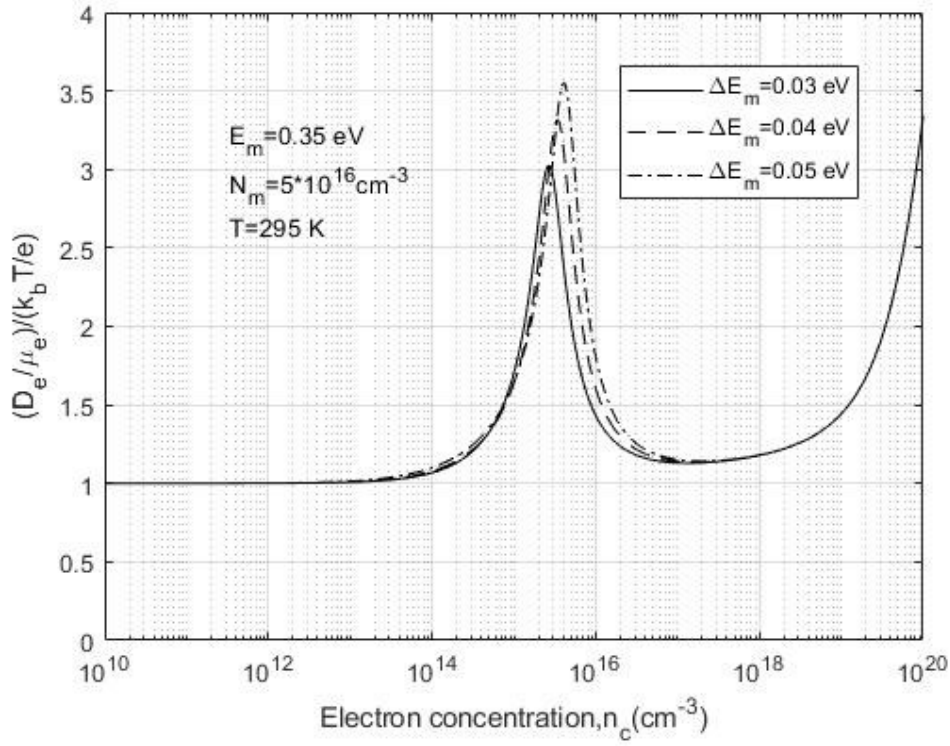


Fig. 4.1: The variation of normalized ratio D_e/μ_e as a function of the free electron concentration for different ΔE_m .

At very low electron concentration, The D_e/μ_e ratio does not have significance impact on varying gaussian width. As we increase gaussian width, D_e/μ_e ratio will increase around $10^{15} \text{ cm}^{-3} \text{ eV}^{-1}$ electron concentration. This shows that the disperse Gaussian distribution in mobility gap will deviate Einstein relation from its unity.

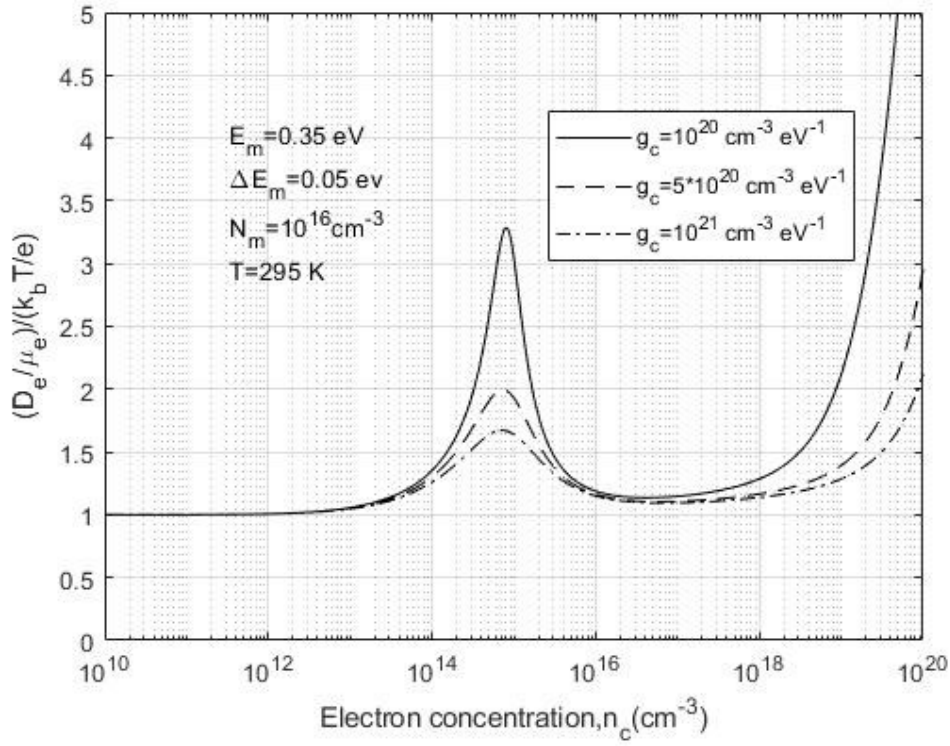


Fig. 4.2: The variation of normalized ratio D_e/μ_e as a function of the free electron concentration for different g_c .

Figure 4.2 shows the effect of g_c on the D_e/μ_e ratio as function of electron concentration. The effect of Gaussian peak increases with decreasing g_c . That means, the relative value of Gaussian states with respect to the extended states has the influence on deviation of ER.

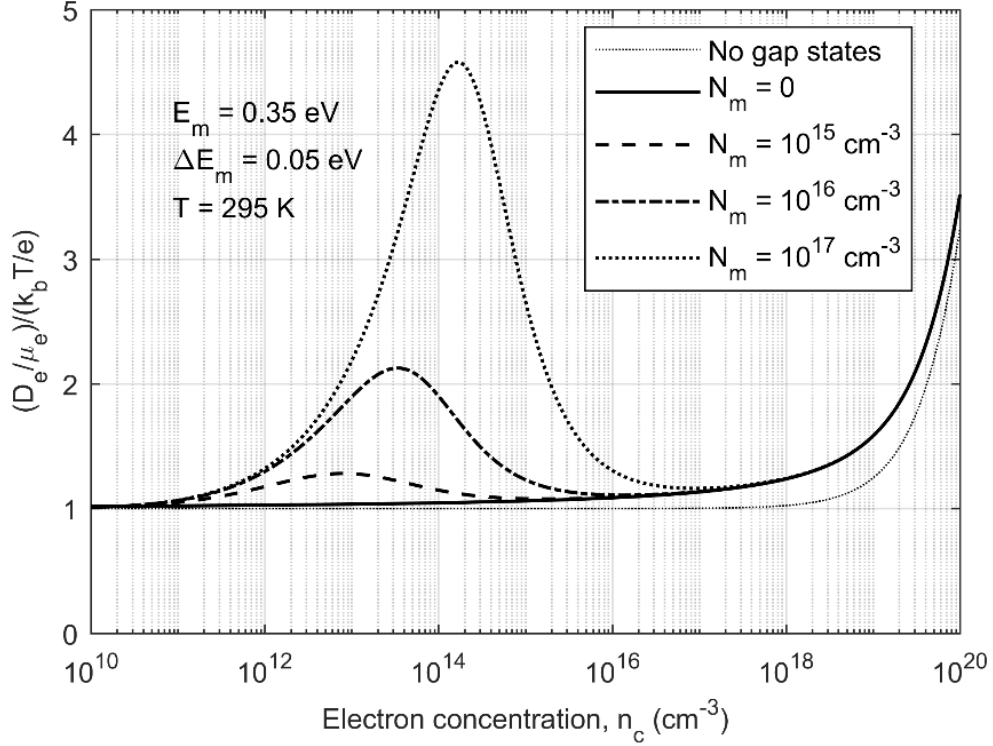


Fig. 4.3: The variation of normalized ratio D_e/μ_e as a function of the free electron concentration for different N_m .

The effects of the location of the Gaussian peak (E_m) in DOS on the D_e/μ_e ratio as a function of the Fermi level is shown in Figure 4.4. The peak in the D_e/μ_e ratio increases with increasing E_m at the same N_m (Figure 4.3). Note that, the peak in the D_e/μ_e ratio is non-existent when E_m is ~ 0.2 eV or less, which signifies that the closer the Gaussian peak to the mobility edge having the same N_m , the lesser the existence of Gaussian peak as compared to the exponential band tail. However, with the increase in E_m , the peak starts to form and increase, signifying that the further the Gaussian peak from band edges, the more significant the impact around the same electron concentration.

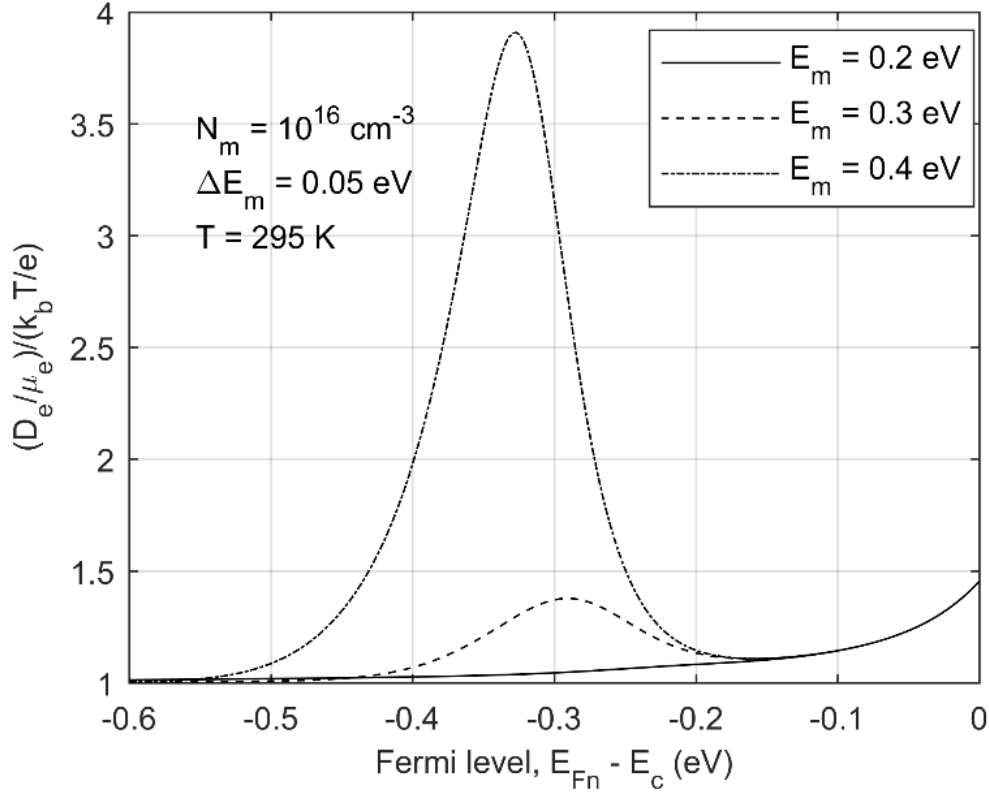


Fig. 4.4: The variation of the normalized ratio D_e/μ_e with the Fermi-level for different positions of Gaussian peak near conduction band.

The Einstein relation for electrons considering usual DOS values from Table I is plotted. Note that Abkowiz [23] has found only one Gaussian peak, whereas, later, other researchers have found two Gaussian peaks near conduction band and their energy positions are quite similar. Therefore, it has been shown the GER for electrons using two sets of parameters from ref - [23] and [17] in Figure 4.5. It has been taken $E_m = 0.35$ eV, $N_m = 10^{16} \text{ eV}^{-1}\text{cm}^{-3}$, $\Delta E_m = 0.05$ eV and $g_c = 10^{20} \text{ cm}^{-3}$ for the curve marked as Abkowiz [23]. Following parameters are taken for two Gaussian peaks in DOS proposed by Kasap *et al.* [17]: $N_{m1} = 5 \times 10^{17} \text{ eV}^{-1}\text{cm}^{-3}$, $E_{m1} = 0.3$ eV, $\Delta E_{m1} = 0.04$ eV; $N_{m2} = 5 \times 10^{15} \text{ eV}^{-1}\text{cm}^{-3}$, $E_{m2} = 0.45$ eV, $\Delta E_{m2} = 0.06$ eV and $g_c = 2 \times 10^{21} \text{ cm}^{-3}$.

³. In both curves, the deviation of Einstein relation from traditional value is noticeable for electron concentration higher than 10^{10} cm^{-3} .

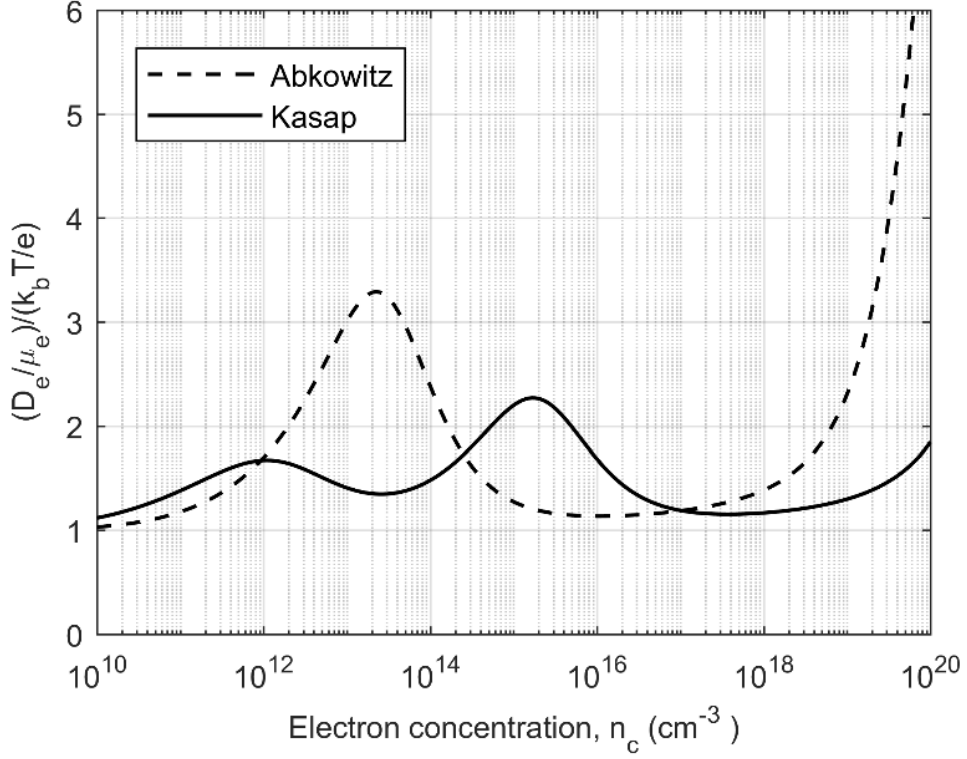


Fig. 4.5: The variation on normalized D_e/μ_e ratio with electron concentration using parameters specified by Abkowitz [23] and Kasap *et al.* [17].

Also, the Einstein relation for holes considering usual DOS values from Table II have been plotted. Note that Abkowitz [23] has found only one Gaussian peak but Kasap *et al.* [17] haven't found any remarkable peak whereas Benkhedir *et al.* [18] have found two Gaussian peaks near valence band. Therefore, it have been shown the GER for holes using two sets of parameters from refs [23] , [18] in Figure 4.6 It has been taken $E_m = 0.27 \text{ eV}$, $N_m = 10^{16} \text{ eV}^{-1}\text{cm}^{-3}$, $\Delta E_m = 0.05 \text{ eV}$ and $g_v = 10^{20} \text{ cm}^{-3}$ for the curve marked as Abkowitz. [23] Following parameters are taken for two Gaussian peaks in DOS proposed by Benkhedir *et al.* [18] $N_{m1} = 5 \times 10^{17} \text{ eV}^{-1}\text{cm}^{-3}$, $E_{m1} =$

0.2 eV, $\Delta E_{m1} = 0.05$ eV, $N_{m2} = 5 \times 10^{15}$ eV⁻¹cm⁻³, $E_{m2} = 0.4$ eV, $\Delta E_{m2} = 0.05$ eV and $g_v = 4 \times 10^{20}$ cm⁻³.

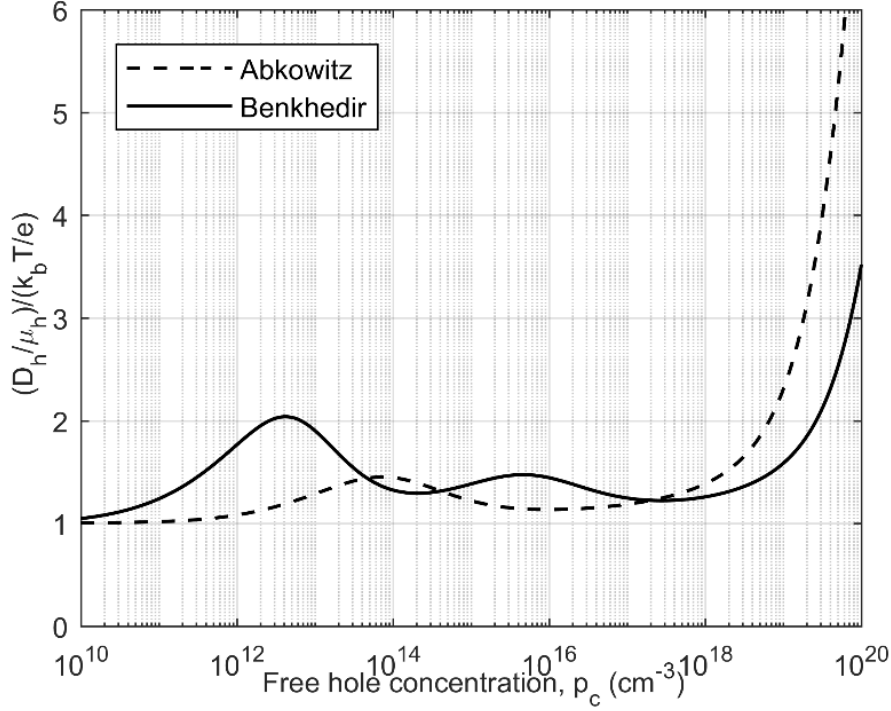


Fig. 4.6: The variation on normalized D_h/μ_h ratio with hole concentration using parameters specified by Abkowitz [23] and Benkhedir *et al.* [18].

The deviation in Einstein relation from conventional relation for electrons is more prominent than that for holes. Because the amount of Gaussian distributed shallow defect states near conduction bands is larger than that of defect states near valence bands. The mobility of electrons is more affected by the shallow states than that of holes [37]. As evident from Figures 4.1 to 4.6, the Einstein relation almost follows the traditional value if the carrier concentration is less than 10^{10} cm⁻³. The Gaussian peaks in the mobility gap have a substantial effect on Einstein relation if the carrier concentration exceeds 10^{10} cm⁻³. The Einstein relation is one to three times more than

the conventional value at moderate carrier concentration of 10^{10} to 10^{14} cm^{-3} . Therefore, this deviation should be considered in more accurate device modeling.

4.3 Field-Diffusion Under Quasi-Equilibrium Transport

The field-diffusion coefficient of electrons and holes in a-Se are examined considering one Gaussian peak in the DOS of near band states. Note that limit of numerical integral of equation edit is considered just to include all shallow trap levels. Figure 4.7 shows the field-diffusion coefficient of electrons in a-Se as a function of electron concentration for different Electric field. The following DOS parameters are assumed for electrons: $E_m = 0.35$ eV, $N_m = 10^{16}$ $\text{eV}^{-1}\text{cm}^{-3}$, $\Delta E_m = 0.05$ eV and $g_c = 4 \times 10^{20}$ cm^{-3} [36]. The field diffusion coefficient is almost constant up to the carrier concentration of 10^{12} cm^{-3} and decreases abruptly with increasing carrier concentration. The field-diffusion coefficient becomes negligibly small when carrier concentration is higher than 10^{15} cm^{-3} . The carrier transport quickly reaches equilibrium with increasing carrier concentration through trap saturation and release events, and thus the field diffusion vanishes. Figure 4.8 shows the total normalized diffusion (thermal + field) coefficient of electrons as a function of electric field at three different carrier concentrations. The normalized field diffusion coefficient increases abruptly at low field and then remains almost stable for the electric field higher than 40 $\text{V}/\mu\text{m}$.

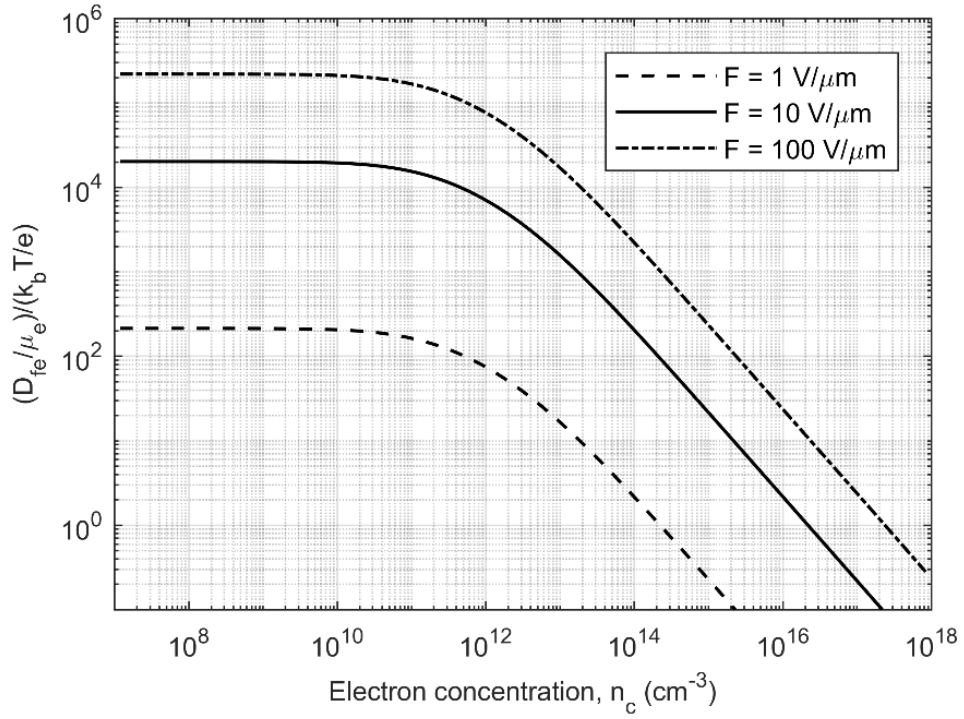


Fig. 4.7: Normalized field-diffusion coefficient of electrons in a-Se as a function of electron concentration at three different electric fields.

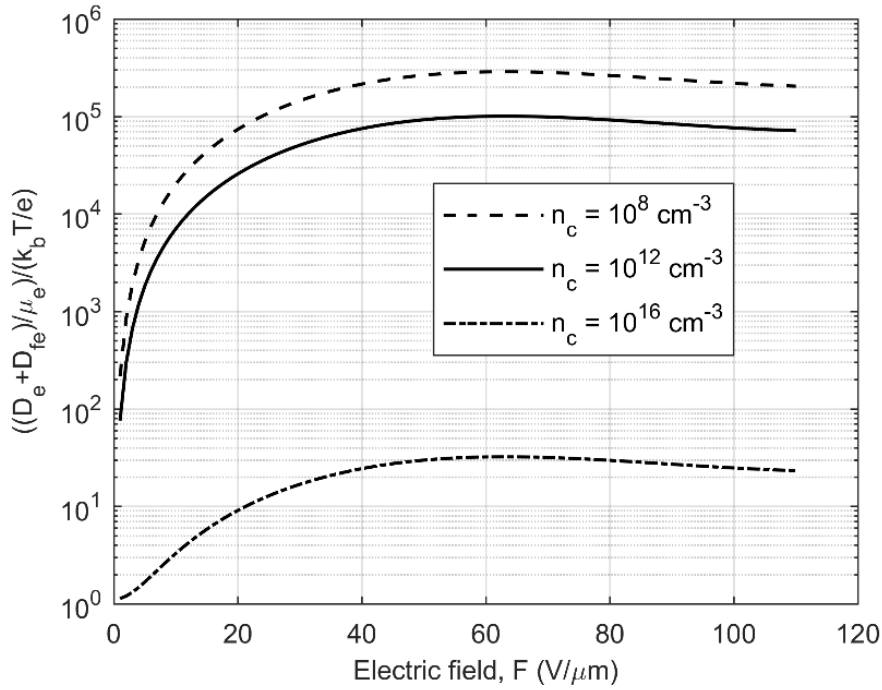


Fig. 4.8: Normalized total diffusion coefficient of electrons in a-Se as a function of electric field at three different electron concentrations.

Figure 4.9 shows the field-diffusion coefficient of holes in a-Se as a function of hole concentration. The following DOS parameters are assumed for holes: $E_m = 0.27$ eV, $N_m = 10^{16}$ eV⁻¹cm⁻³, $\Delta E_m = 0.05$ eV and $g_v = 4 \times 10^{20}$ cm⁻³ [36]. Figure 4.10 the total normalized diffusion (thermal + field) coefficient of holes as a function of electric field at three different carrier concentrations. The results of holes are similar to that of electrons because of similar DOS parameters.

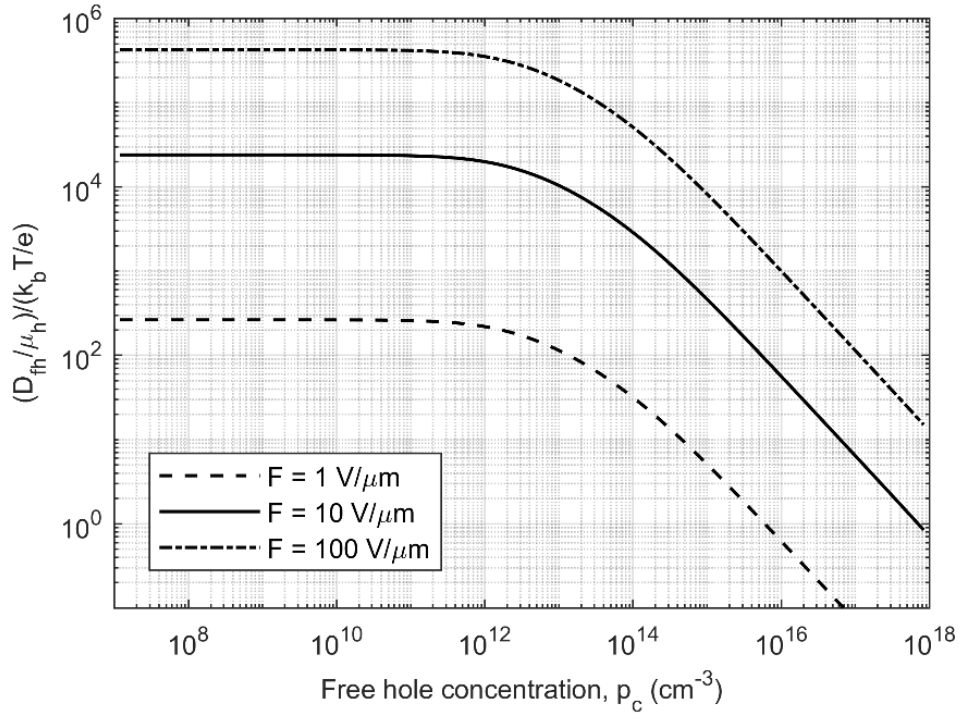


Fig. 4.9: Normalized field-diffusion coefficient of holes in a-Se as a function of hole concentration at three different electric fields.

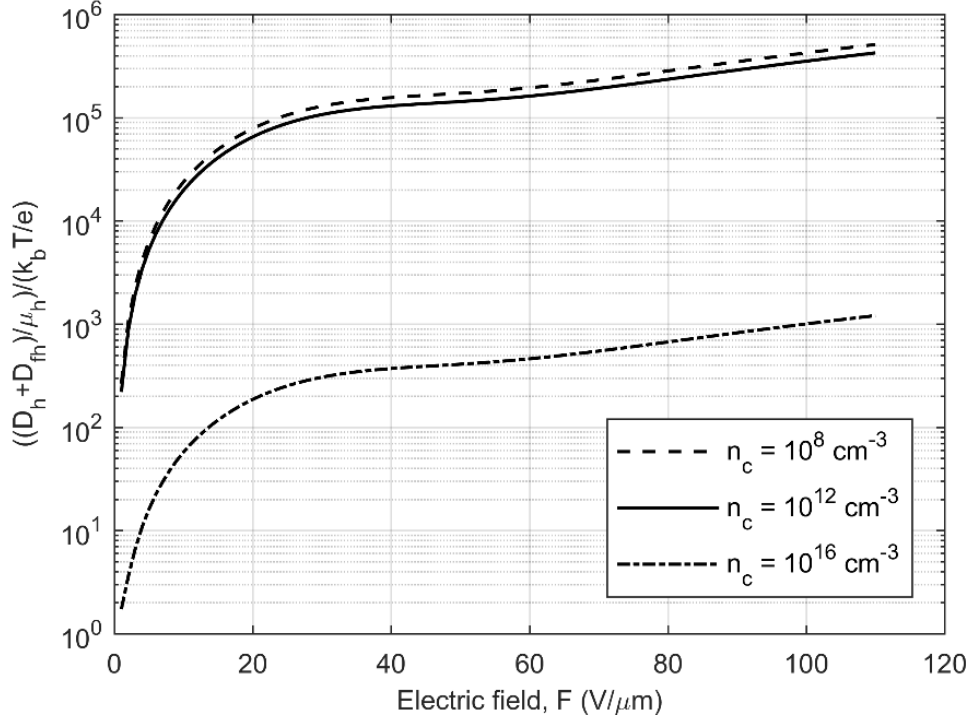


Fig. 4.10: Normalized total diffusion coefficient of holes in a-Se as a function of electric field at three different hole concentrations.

4.4 Conclusion

Due to the defect states of a-Se, ER deviates from its unity value when carrier concentration is larger than 10^{10} cm^{-3} . The deviation of ER also strongly depends on the variation in DOS parameters including the position, width, and carrier concentration of Gaussian distribution, with an increase of ER noted with the increase of each of the Gaussian parameter.

The field diffusion coefficient of a-Se depends on electric field as well as carrier concentration. At a carrier concentration lower than 10^{12} cm^{-3} , the field diffusion coefficient is almost constant. With higher carrier concentration, the field diffusion coefficient starts decreasing and after 10^{15} cm^{-3} it becomes almost non-existent.

Chapter 5: Conclusions and Contributions

5.1 Conclusions

This thesis work has analyzed the generalized Einstein relation for DOS in a-Se that consists of square-root distribution for extended band states and summation of exponential and the Gaussian distributions for tail states close to the mobility edges. The effects of the DOS parameters on the Einstein relationship as a function of carrier concentration has been analysed. The results show that the diffusivity-mobility ratio for such DOS distribution substantially deviates from traditional constant value for carrier concentration larger than 10^{10} cm^{-3} and strongly depends on the amount, energy position, and the shape of the Gaussian peaks. The diffusion coefficient of charge carriers obtained from Einstein relation is valid at thermal equilibrium or at a very low electric field under small signal. This thesis work also analyzed the field diffusion coefficient of electrons and holes in a-Se, which is found to strongly dependent on the electric field and carrier concentration. It increases with electric field but decreases with increasing carrier concentration.

5.2 Contributions

The contributions of this thesis work can be summarized below:

- Developed a theoretical model for analysing the generalized Einstein relation in amorphous semiconductors at thermal equilibrium with a particular application to amorphous selenium.
- The effects of different DOS parameters on GER are analyzed.
- A new field-induced diffusion coefficient for amorphous semiconductors was introduced which depends on both the electric field and carrier concentration.

- The effects of electric field and carrier concentration on field-diffusion coefficient was investigated.

5.3 Future works

It would be very conclusive if the theoretical results could be verified with the experimental measurement. Unfortunately, no experimental data was available in literature. This could a potential future work. The analytical and semi-analytical work of this thesis can also be verified with Monte Carlo simulation considering the true carrier dynamics.

5.4 Publication

Dilshad Hossain, M.Z. Kabir, "Diffusion coefficient of charge carriers in disordered semiconductors retaining a combination of exponential and Gaussian mobility-gap states: Application to amorphous selenium", *Journal of Vacuum Science & Technology B*, vol 39, no 6, pp 062211, 2021.

References

- [1] T. Jenkins, " A brief history of semiconductors," *Physics education*, vol. 40, no. 5, p. 430, 2005.
- [2] D. A. Neamen, "Semiconductor Physics and Devices Basic Principles," McGraw-Hill, 2003.
- [3] M. Shur, "Physics of Semiconductor Devices," Prentice Hall Series in Solid State Physical Electronics-Nick Holonyak, Jr. Editor, 1990.
- [4] B. Streetman *et al.*, "Solid State Electronic Devices," Harlow, Essex : Pearson Education Limited, 2016.
- [5] C. J. Haugen, "Charge Transport in Stabilized a-Se Films Used in X-ray image detector application ," PhD thesis, University of Saskatchewan, 1998.
- [6] V. I. Arkhipov *et al.*, "Charge Transport in Disordered Organic Semiconductors," in *Photophysics of Molecular Materials*, WILEY-VCH Verlag GmbH & Co. KGaA, 2006, p. 267.
- [7] M. Madan *et al.*, "The Physics and Applications of Amorphous Semiconductors," Elsevier, 1988.
- [8] N. F. Mott, " Electrons in disordered structures," *Advances in Physics*, vol. 16, no. 61, pp. 49-144, 1967.
- [9] P. W. Anderson, "Absence of Diffusion in Certain Random Lattices," *Physical Review*, vol. 109, no. 5, pp. 1492-1505, 1958.

- [10] A. E. Owen *et al.*, "Drift mobility studies in vitreous arsenic triselenide," *The Philosophical Magazine*, vol. 24, no. 192, pp. 1281-1290, 1971.
- [11] M. H. Cohen *et al.*, "Simple band model for amorphous semiconducting alloys.," *Physical review letters*, vol. 22, no. 20, pp. 1065-1068, 1969.
- [12] Y. Roichman, Y. Preezant and N. Tessler, "Analysis and modeling of organic devices," *physica status solidi (a)*, vol. 201, no. 6, pp. 1246-1262, 2004.
- [13] R. Richert *et al.*, "Diffusion and drift of charge carriers in a random potential: Deviation from Einstein's law," *Phys. Rev. Lett.*, vol. 63, no. 5, pp. 547-550, 1989.
- [14] L. Pautmeier *et al.*, "Anomalous time-independent diffusion of charge carriers in a random potential under a bias field," *Philosophical Magazine B: Physics of Condensed Matter; Statistical Mechanics, Electronic, Optical and Magnetic Properties*, vol. 63, no. 3, pp. 587-601, 1991.
- [15] M. Borsenberger *et al.*, "Dispersive and nondispersive charge transport in a molecularly doped polymer with superimposed energetic and positional disorder," *Phys. Rev. B*, vol. 47, no. 8, pp. 4289--4295, 1993.
- [16] K. Koughia *et al.*, "Density of localized electronic states in *a*-Se from electron time-of-flight photocurrent measurements," *Journal of Applied Physics*, vol. 97, no. 3, p. 033706, 2005.
- [17] S. Kasap *et al.*, "Charge transport in pure and stabilized amorphous selenium: Re-examination of the density of states distribution in the mobility gap and the role of defects," *J. Mater. Sci.: Mater. Electron.*, vol. 26, no. 7, pp. 4644-4658, 2015.

- [18] M. L. Benkhedir *et al.*, "Structure of the band tails in amorphous selenium.," *Journal of Physics: Condensed Matter*, vol. 20, no. 21, p. 215202, 2008.
- [19] N.Hijazi *et al.*, "Temperature and field dependent effective hole mobility and impact ionization at extremely high fields in amorphous selenium," *Applied Physics Letters* , vol. 104, no. 19, p. 192103, 2014.
- [20] T.H Nguyen, " Einstein relation for disordered semiconductors: A dimensionless analysis.," *J. Appl. Phys.*, vol. 98, no. 7, p. 076102 , 2005.
- [21] Y. Wei *et al.*, "Generalized Einstein relation for co-doped organic semiconductors," *Journal of Applied Physics*, vol. 118, no. 12, p. 125501, 2015.
- [22] T. Mehmetolu *et al.*, "Full Analytical Evaluation of the Einstein Relation for Disordered Semiconductors," *IEEE Transactions on Electron Devices*, vol. 62, no. 5, pp. 1580-1583, 2015.
- [23] M. Abkowitz, "Density of states in a-Se from combined analysis of xerographic potentials and transient transport data," *Philosophical magazine letters*, vol. 58, no. 1, pp. 53-57, 1988.
- [24] H. Huang *et al.*, "Recent developments of amorphous selenium-based X-ray detectors: a review.," *IEEE Sensors Journal* , vol. 20, no. 4, pp. 1694-1704, 2020.
- [25] S. O. Kasap *et. al.*, "Erratum: "Effects of x-ray irradiation on charge transport and charge collection efficiency in stabilized a-Se photoconductors," *Journal of Applied Physics*, vol. 127, no. 8, p. 084502, 2020.

- [26] W. Smith, *Nature* (London), vol. 7, no. 170, p. 303, 1873.
- [27] J. Mort, *Anatomy of Xerography*, London: McFairland and Co, 1989.
- [28] S. O. Kasap *et al.*, "Amorphous selenium and its alloys from early xeroradiography to high resolution X-ray image detectors and ultrasensitive imaging tubes," *Physica status solidi (b)*, vol. 246, no. 8, pp. 1794-1805, 2009.
- [29] H. Naito *et al.*, "Computer simulation study of tail-state distribution in amorphous selenium," *Journal of Non-Crystalline Solids*, vol. 114, pp. 112-114, 1989.
- [30] J. A. Rowlands *et al.*, "Review X-ray photoconductors and stabilized a-Se for direct conversion digital flat-panel X-ray image-detectors," *Journal of materials science: materials in electronics*, vol. 11, no. 3, pp. 179-198, 2000.
- [31] L Li *et al.*, "General Einstein relation model in disordered organic semiconductors under quasiequilibrium," *Physical Review B*, vol. 90, no. 21, p. 214107, 2014.
- [32] V. I. Arkhipov *et al.*, "Drift and diffusion in materials with traps," *Philosophical Magazine B*, vol. 45, no. 2, pp. 177-187, 1982.
- [33] A. Y. Kudrov *et al.*, "Field diffusion in disordered organic materials under conditions of occupied deep states," *Semiconductors*, vol. 51, p. 158-162, 2017.
- [34] S. O. Kasap *et al.*, "Time-of-flight drift mobility measurements on chlorine-doped amorphous selenium films," *Journal Physics D: Applied Physics*, vol. 18, no. 4, p. 703, 1985.

- [35] Nir Tessler *et al.*, "Amorphous organic molecule/polymer diodes and transistors— Comparison between predictions based on Gaussian or exponential density of states," *Organic Electronics*, vol. 6, pp. 200-210, 2005.
- [36] M. Z. Kabir *et al.*, "Mechanisms of temperature-and field-dependent effective drift mobilities and impact ionization coefficients in amorphous selenium," *Canadian Journal of Physics*, vol. 93, no. 11, pp. 1407-1412, 2015.
- [37] G Juška *et al.*, "Impact ionization and mobilities of charge carriers at high electric fields in amorphous selenium," *physica status solidi (a)*, vol. 59, no. 1, pp. 389-393, 1980.
- [38] J. A. Rowlands *et. al.*, "Direct-conversion flat-panel X-ray image sensors for digital radiography," *Proceedings of the IEEE*, vol. 90, no. 4, pp. 591-604, 2002.
- [39] O. Bubon *et. al.*, "Amorphous selenium (a-Se) avalanche photosensor with metal electrodes," *Journal of non-crystalline solids* , vol. 358, no. 17, pp. 2431-2433, 2012.